ABSTRACT

CYCLIC PREFIX ASSISTED BLOCK TRANSMISSION FOR LOW COMPLEXITY COMMUNICATION SYSTEM DESIGN

by
Haibin Huang

This thesis presents new results on cyclic prefix (CP) assisted block transmission for *low complexity* communication system design. Two important aspects are studied: the CP based low-complexity schemes for channel equalization and channel estimation.

Specifically, based on the simple frequency domain equalization, a low complexity joint receiver is proposed for CP-CDMA system, which is a special application of block transmission.

And in this work the finite impulse response (FIR) model is used for the unknown communication channels. To identify an unknown FIR channel, a novel channel estimation method is proposed by exploiting the cyclic prefix technique. Compared to a conventional method, the proposed method delivers the similar estimation accuracy, yet at much lower system overhead and lower computational complexity. In order to minimize the channel total mean square error in channel estimation, the criteria and solutions to optimal training sequence design are also presented. Finally, the performance study is carried out on the proposed channel estimation scheme for BPSK block transmission system as well as CP-CDMA system using simulation along with analysis.

CYCLIC PREFIX ASSISTED BLOCK TRANSMISSION FOR LOW COMPLEXITY COMMUNICATION SYSTEM DESIGN

by
Haibin Huang

A Thesis
Submitted to the Faculty of
New Jersey Institute of Technology
in Partial Fulfillment of the Requirements for the Degree of
Master of Science in Electrical Engineering

Department of Electrical and Computer Engineering

January 2005

Blank Page

APPROVAL PAGE

CYCLIC PREFIX ASSISTED BLOCK TRANSMISSION FOR LOW COMPLEXITY COMMUNICATION SYSTEM DESIGN

Haibin Huang

Dr. Hongya Ge, Thesis Advisor Date
Associate Professor of Electrical and Computer Engineering, NJIT

Dr., Ali Abdi Date
Assistant Professor of Electrical and Computer Engineering, NJIT

Dr., Roy R. You Date
Assistant Professor of Electrical and Computer Engineering, NJIT

BIOGRAPHICAL SKETCH

Author: Haibin Huang

Degree: Master of Science

Date: January 2005

Undergraduate and Graduate Education:

- Master Degree of Engineering,
  Xidian University, Xi'an, China, 1999

- Bachelor Degree of Engineering,
  Xidian University, Xi'an, China, 1996

Major: Electrical Engineering

Dedicated to my beloved parents, wife and daughter

谨献给我深爱的父母，妻子和女儿

ACKNOWLEDGMENT

I would like to express my deep appreciation to Dr. Hongya Ge for her valuable suggestions and kind assistance throughout the writing of this thesis. Special thanks are given to Dr. Ali Abdi and Dr. Roy R. You for actively participating in my committee.

My colleagues in the Center for Communications and Signal Processing Research also deserve acknowledgment for their help.

Most of all, I would like to thank my beloved parents, wife and daughter. Without them, I could not go through this journey smoothly.

TABLE OF CONTENTS

TABLE OF CONTENTS
(Continued)

LIST OF TABLES

LIST OF FIGURES

LIST OF FIGURES
(Continued)

LIST OF SYMBOLS

$\mathbf{A}^T$: Transpose of $\mathbf{A}$

$\mathbf{A}^H$: Hermition of $\mathbf{A}$

$\mathbf{A}^*$: Complex conjugate of $\mathbf{A}$

$\mathrm{Re}(\mathbf{A})$: Real part of A

$E(\mathbf{A})$: Expectation of $\mathbf{A}$

$tr(\mathbf{A})$: Trace of $\mathbf{A}$

$diag(\mathbf{a})$: Diagonal matrix whose diagonal elements are specified by vector $\mathbf{a}$

$sign(\mathbf{A})$: A matrix whose elements are the signs of the corresponding elements of $\mathbf{A}$

$\mathbb{R}^{m\times n}$: A linear space consisting of real-valued matrices of dimension m×n

$\mathbb{C}^{m\times n}$: A linear space consisting of complex-valued matrices of dimension m×n

CHAPTER 1

INTRODUCTION

Cyclic prefix (CP) assisted block transmission is an efficient communication scheme over time-dispersive channels. Such technique has been successfully applied to the multi-carrier based orthogonal frequency division multiplexing (OFDM) systems. It improves the spectrum utilization and simplifies the channel equalization at the receiver through frequency domain processing.

For the downlink application of DS-CDMA systems, information bits from multiple users can be spread by orthogonal Walsh codes. However, propagation through a time-dispersive multipath channel destroys the orthogonality between different spreading codes (signatures). Such loss of code orthogonality gives rise to the multiple access interference (MAI) and inter-symbol-interference (ISI), hence degrades detection performance. A conventional method to combat distortion and utilize multipath components is the RAKE receiver, which uses a bank of path matched-filters (fingers) to individually process multiple delayed versions of signal component and combine the outputs based on some combining criterions. Essentially, the conventional RAKE receiver is a single user receiver making use of multipath components while ignoring the MAI from other existing users. The other solution is the multiuser detector (MUD), which jointly considers the structure of all users' signals, resulting in much better performance at the price of higher complexity. But in practice, only the signature of the interested user is available, hence MUD cannot be obtained for downlink detection without relying on the estimated MAI.

The use of CP assisted block transmission in single carrier downlink synchronous DS-CDMA system leads to the CP-CDMA system [1]. Such scheme improves the receiver design in many ways, for example: 1) A simple frequency domain equalizer can be applied instead of the RAKE receiver; 2) Orthogonality of spreading codes will be kept if the channel is known, therefore the single-user detection scheme can be directly used. With a reasonable approximation on the statistics of the transmitted data, we propose a low complexity frequency domain joint receiver consists of block equalization, de-spread and data detection.

In practice, the channel state information (CSI) is not given as a prior knowledge, especially in a time-variant environment. Therefore, the CSI must be estimated before equalization and subsequent coherent detection. There are basically two kinds of estimation schemes: training based channel estimation, in which a known training sequence is transmitted periodically; and blind channel estimation, in which training sequence is not needed but the higher order statistics (HOS) or second order statistics (SOS) are needed. Compared to blind channel estimation, training based channel estimation has much lower complexity but with additional system overhead. This work concentrates on the training based estimation approaches for block transmission. The proposed method, compared to the conventional method [7], has lower system overhead and lower complexity but similar estimation accuracy.

This thesis is organized as follows: Chapter 2 reviews the time domain equalization and frequency domain equalization methods based on the zero-forcing (ZF) and the minimum mean square error (MMSE) criterions. A low complexity frequency domain joint receiver for CP-CDMA system is proposed in Chapter 3. In Chapter 4, a novel channel estimation method based on cyclic prefix is proposed for CP assisted block transmission, along with the design of optimal training sequence. Lastly, we study the performance of the proposed solution in the BPSK block transmission system and the CP-CDMA system through simulation and analysis.

CHAPTER 2

CYCLIC PREFIX ASSISTED BLOCK TRANSMISSION

Throughout this chapter, the channel is known to the receiver. Firstly the time domain and frequency domain equalizers are derived based on zero-forcing (ZF) as well as linear MMSE criterions, respectively. To be simple, the abbreviations TEQ and FEQ are used to denote the time domain equalizer and the frequency domain equalizer, respectively. Then the equivalence of ZF-TEQ (or MMSE-TEQ) and ZF-FEQ (or MMSE-FEQ) is shown.

Lastly, the MSE and BER performances of ZF equalizer as well as MMSE equalizer are studied for the BPSK block transmission system.

2.1 Signal Model

The frame structure of cyclic prefix assisted block transmission is shown in Figure 2.1.

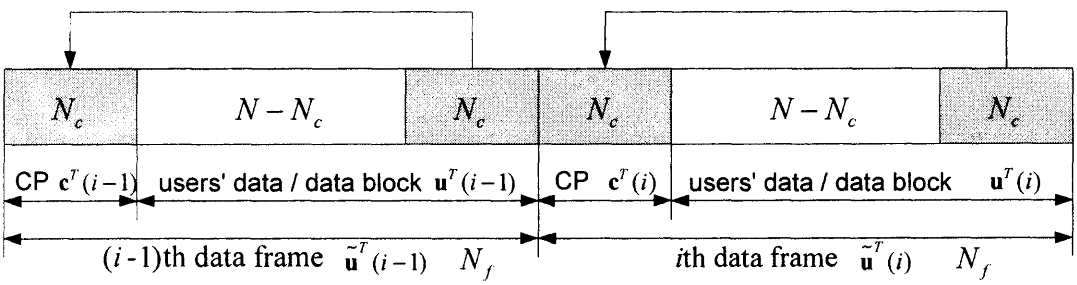

Figure 2.1 Frame structure of cyclic prefix assisted block transmission.

The ith frame is denoted by $\tilde{\mathbf{u}}(i) = [\tilde{u}(iN_f), ..., \tilde{u}((i+1)N_f - 1)]^T = [\mathbf{c}^T(i), \mathbf{u}^T(i)]^T$, where $\mathbf{u}(i)$ denotes the users' data block and the CP $\mathbf{c}(i)$ is simply the copy of the last N_c elements of $\mathbf{u}(i)$. And the matrix form is $\tilde{\mathbf{u}}(i) = \mathbf{T}_{in}\mathbf{u}(i)$, where $\mathbf{T}_{in} = [\tilde{\mathbf{I}}^T_{N_c \times N}, \mathbf{I}_N]^T$ is defined as an inserting matrix with $\tilde{\mathbf{I}}_{N_c \times N} = [0_{N_c \times (N-N_c)}, \mathbf{I}_{N_c}]$.

Assume a symbol rate processing at the receiver, the discrete-time dispersive channel can be modeled by a vector $\mathbf{h} = [h(0), \cdots, h(L)]^T$ whose length does not exceed some known constant $(L+1)$. Note that $\mathbf{h}$ represents a combined discrete impulse response of the transmit pulse shaping filter, the delay-spread channel and the receive pulse shaping filter. Throughout, $(L+1) \ll N$ is assumed.

At symbol rate, the nth sample of received data can be modeled as

$$\tilde{r}(n) = \sum_{l=0}^{L} h(l)\, \tilde{u}(n-l) + v(n) \tag{2.1}$$

where $v(n)$ is assumed to be the additive white Gaussian noise (AWGN) with zero mean and variance σ_v^2. And the noise, the source data and the possibly random channel coefficients are further assumed to be statistically independent.

For the ith frame, the N_f received samples can be collected into a data vector $\tilde{\mathbf{r}}(i) = [\tilde{r}(iN_f), ..., \tilde{r}((i+1)N_f - 1)]^T$. Then

$$\tilde{\mathbf{r}}(i) = \widetilde{\mathbf{H}}_0 \tilde{\mathbf{u}}(i) + \widetilde{\mathbf{H}}_1 \tilde{\mathbf{u}}(i-1) + \tilde{\mathbf{v}}(i) \tag{2.2}$$

where $\widetilde{\mathbf{H}}_0 \in \mathbb{C}^{N_f \times N_f}$ is a lower triangle Toeplitz matrix with its first column specified by

$[h(0),\ldots,h(L),0,\ldots,0]^T$, and $\widetilde{\mathbf{H}}_1 \in \mathbb{C}^{N_f \times N_f}$ is an upper triangle Toeplitz matrix with its last column specified by $[h(1),\ldots,h(L),0,\ldots,0]^T$. That is,

$$\widetilde{\mathbf{H}}_0 = \begin{bmatrix} h(0) & 0 & 0 & \cdots & 0 \\ \vdots & h(0) & 0 & \cdots & 0 \\ h(L) & \cdots & \ddots & \ddots & \vdots \\ \vdots & \ddots & \cdots & \ddots & 0 \\ 0 & \cdots & h(L) & \cdots & h(0) \end{bmatrix} \tag{2.3}$$

and

$$\widetilde{\mathbf{H}}_1 = \begin{bmatrix} 0 & \cdots & h(L) & \cdots & h(1) \\ \vdots & 0 & 0 & \ddots & \vdots \\ 0 & \cdots & \ddots & \ddots & h(L) \\ \vdots & \ddots & \cdots & \ddots & 0 \\ 0 & \cdots & 0 & \cdots & 0 \end{bmatrix} \tag{2.4}$$

It is easy to see from Equation (2.2) that the inter-block-interference (IBI) between the successive blocks arises due to the dispersive nature of the channel. To completely cancel the IBI, $N_c \geq L+1$ is required. And $N_c = L+1$ is chosen in the sequel.

After discarding the CP, the remaining received N samples corresponding to the ith data block are

$$\begin{aligned} \mathbf{r}(i) &= \mathbf{T}_b \tilde{\mathbf{r}}(i) \\ &= \mathbf{T}_b \widetilde{\mathbf{H}}_0 \tilde{\mathbf{u}}(i) + \mathbf{T}_b \widetilde{\mathbf{H}}_1 \tilde{\mathbf{u}}(i-1) + \mathbf{T}_b \tilde{\mathbf{v}}(i) \end{aligned} \tag{2.5}$$

where $\mathbf{T}_b = [0_{N\times N_c}, \mathbf{I}_N]$ is designed to delete the CP part in the received data frame. Hence, $\mathbf{T}_b \widetilde{\mathbf{H}}_1 = \mathbf{0}_{N\times N_f}$ and

$$\mathbf{T}_b\widetilde{\mathbf{H}}_0 = \begin{bmatrix} 0 & h(L) & \cdots & h(0) & 0 & \cdots & 0 \\ \vdots & \ddots & \ddots & \ddots & \ddots & \ddots & \vdots \\ \vdots & \ddots & \ddots & \ddots & \ddots & \ddots & 0 \\ 0 & \cdots & \cdots & 0 & h(L) & \cdots & h(0) \end{bmatrix}_{N\times N_f}$$

Since $\tilde{\mathbf{u}}(i) = \mathbf{T}_{in}\mathbf{u}(i)$, the simple linear model can be obtained if the frame index is ignored without loss of generality

$$\mathbf{r} = \mathbf{H}_r\mathbf{u} + \mathbf{v} \tag{2.6}$$

where $\mathbf{v}$ is still AWGN with zero mean and covariance matrix $\sigma_v^2\mathbf{I}_N$ $\mathbf{H}_r \in \mathbb{C}^{N\times N}$ is a circulant square matrix, i.e.,

$$\mathbf{H}_r = \begin{bmatrix} h(0) & 0 & \cdots & 0 & h(L) & \cdots & h(1) \\ \vdots & \ddots & \ddots & & \ddots & \ddots & \vdots \\ \vdots & & & & & \ddots & h(L) \\ h(L) & \ddots & & \ddots & & & 0 \\ 0 & \ddots & \ddots & & & \ddots & \vdots \\ \vdots & \ddots & \ddots & \ddots & & \ddots & 0 \\ 0 & \cdots & 0 & h(L) & \cdots & \cdots & h(0) \end{bmatrix} \tag{2.7}$$

To perform linear equalization in block sense, the linear equalizer matrix is denoted by $\mathbf{W} \in \mathbb{C}^{N\times N}$ such that

$$\hat{\mathbf{u}} = \mathbf{W}^H\mathbf{r} \tag{2.8}$$

where $\hat{\mathbf{u}}$ is the estimate of $\mathbf{u}$. And the corresponding MSE for the whole data block in time domain is defined as

$$\xi_T = E\{\| \mathbf{u} - \hat{\mathbf{u}} \|^2\} \tag{2.9}$$

2.2 Time Domain Equalization

Although there are many time domain approaches to deal with the estimation problem in Equation (2.6), only the time domain approaches based on the ZF and the linear MMSE criteria are considered. In this section, the circulant structure of $\mathbf{H}_r$ is not utilized.

2.2.1 Zero-Forcing Time Domain Equalizer

The standard solution is

$$\mathbf{W}_{ZF-TEQ} = (\mathbf{H}_r^{-1})^H \tag{2.10}$$

when the square matrix $\mathbf{H}_r$ is full rank. Therefore the ZF-TEQ has a limitation to recover symbols if such condition is broken. However, its advantage is that the statistics of the additive noise and source data are not required.

The main drawback of the ZF solution is the noise enhancement on signal components located at the low response region of the channel frequency response. To alleviate such drawback, the linear MMSE solution will be introduced as follows.

2.2.2 MMSE Time Domain Equalizer

Given the statistics of the additive noise and users' data, a better equalizer can be achieved in the sense of minimizing the MSE under linear constraint. Based on Equations (2.8) and (2.9), the MSE can be specified by

$$\xi_T = tr(\mathbf{R}_u) + tr(\mathbf{W}^H \mathbf{R}_r \mathbf{W}) - 2\,\mathrm{Re}[tr(\mathbf{W}^H \mathbf{R}_{ru})] \tag{2.11}$$

where $\mathbf{R}_u = E(\mathbf{u}\mathbf{u}^H)$, $\mathbf{R}_r = E(\mathbf{r}\mathbf{r}^H)$ and $\mathbf{R}_{ru} = E(\mathbf{r}\mathbf{u}^H)$ are the auto correlation and cross-correlation matrices. For the model shown in Equation (2.6), their expressions are

$$\mathbf{R}_r = \sigma_v^2 \mathbf{I}_N + \mathbf{H}_r \mathbf{R}_u \mathbf{H}_r^H \tag{2.12}$$

$$\mathbf{R}_{ru} = \mathbf{H}_r \mathbf{R}_u \tag{2.13}$$

Minimizing ξ_T leads to the MMSE solution

$$\mathbf{W}_{MMSE-TEQ} = \mathbf{R}_r^{-1} \mathbf{R}_{ru} \tag{2.14}$$

whose specific form is

$$\mathbf{W}_{MMSE-TEQ} = \left(\sigma_v^2 \mathbf{I}_N + \mathbf{H}_r \mathbf{R}_u \mathbf{H}_r^H\right)^{-1} \mathbf{H}_r \mathbf{R}_u \tag{2.15}$$

It is easy to see that MMSE-TEQ always exists in noisy environment due to the diagonal loading term from the additive noise contained in the matrix inversion. Hence, it can recovery symbols transmitted over any FIR channel.

2.2.3 Mean Square Error Performance

MSE of ZF-TEQ and MMSE-TEQ can be obtained as follows,

$$\xi_{ZF-TEQ} = \sigma_v^2 tr\left[\left(\mathbf{H}_r^H \mathbf{H}_r\right)^{-1}\right] \tag{2.16}$$

$$\xi_{MMSE-TEQ} = tr\left[\mathbf{R}_u - \mathbf{R}_u \mathbf{H}_r^H \left(\sigma_v^2 \mathbf{I}_N + \mathbf{H}_r \mathbf{R}_u \mathbf{H}_r^H\right)^{-1} \mathbf{H}_r \mathbf{R}_u\right] \tag{2.17}$$

For now, it is not explicit to compare their MSE performance in terms of above expressions, but will be clear in the later analysis in frequency domain.

2.3 Frequency Domain Equalization

Unlike above time domain counterparts, frequency domain methods exploit the circulant structure of $\mathbf{H}_r$ to simplify the matrix inversion.

It is well known that an $N \times N$ circulant matrix $\mathbf{H}_r$ can be eigen-decomposed by a discrete Fourier transform (DFT) matrix, and its eigenvalues are simply the coefficients of DFT vector of the first column of $\mathbf{H}_r$. A unitary N-point DFT matrix is defined as $\mathbf{F}_N = [\mathbf{f}_{N,0}, \ldots, \mathbf{f}_{N,N-1}]^H$, where $\mathbf{f}_{N,n} = \frac{1}{\sqrt{N}}[1, e^{-j2\pi n/N}, \cdots, e^{-j2\pi n(N-1)/N}]^H$.

Consequently, Equation (2.6) can be transformed into frequency domain

$$\mathbf{r}_F = \mathbf{G}\mathbf{u}_F + \mathbf{v}_F \tag{2.18}$$

where $\mathbf{G} = diag(\mathbf{g}) = \mathbf{F}_N \mathbf{H}_r \mathbf{F}_N^H$. Vectors $\mathbf{r}_F, \mathbf{u}_F, \mathbf{v}_F$ and $\mathbf{g}$ respectively denote the N-point DFT vectors of $\mathbf{r}, \mathbf{u}, \mathbf{v}$ and $\mathbf{h}$. Due to the diagonal nature of the matrix $\mathbf{G}$, the set of linear equations in Equation (2.18) can be decoupled into scalar forms, i.e.

$$r_F(k) = g(k)u_F(k) + v_F(k), \qquad k = 0, \cdots, N-1 \tag{2.19}$$

If $x(k)$ is assumed to be a *scalar* FEQ at the kth frequency bin, the estimate of $u_F(k)$ can be obtained as $\hat{u}_F(k) = x^*(k) r_F(k)$. And the corresponding matrix form is $\hat{\mathbf{u}}_F = \mathbf{X}^H \mathbf{r}_F$, where $\hat{\mathbf{u}}_F$ denotes the estimate of $\mathbf{u}_F$ and $\mathbf{X} = diag(x(0), \cdots, x(N-1))$ is the

FEQ matrix. Finally $\mathbf{u}$ can be estimated by $\hat{\mathbf{u}} = \mathbf{F}_N^H \hat{\mathbf{u}}_F = \mathbf{F}_N^H \mathbf{X}^H \mathbf{F}_N \mathbf{r}$, in other words, the FEQ can be expressed by

$$\mathbf{W}_{FEQ} = \mathbf{F}_N^H \mathbf{X} \mathbf{F}_N \tag{2.20}$$

It is interesting to observe that $\mathbf{W}_{FEQ}$ is a reconstructed square matrix whose eigenvalues are the scalar FEQ $\{x(n), n = 0, \cdots, N-1\}$ and eigenvectors are N-point IDFT!

2.3.1 Zero-Forcing Frequency Domain Equalizer

Assume that $\mathbf{h}$ has no zero at all N frequency bins, i.e., $g(k) \neq 0,\ \forall k \in \{0, \cdots, N-1\}$. The scalar ZF-FEQ (cf. Equation (2.19)) is

$$x_{ZF}(k) = 1/g^*(k), \qquad k = 0, \cdots, N\text{-}1 \tag{2.21}$$

Its matrix form is

$$\begin{aligned} \mathbf{X}_{ZF} &= (\mathbf{G}^{-1})^H \\ &= \mathbf{F}_N (\mathbf{H}_r^{-1})^H \mathbf{F}_N^H \end{aligned} \tag{2.22}$$

then (cf. Equation (2.18))

$$\mathbf{W}_{ZF-FEQ} = (\mathbf{H}_r^{-1})^H \tag{2.23}$$

Namely, ZF-FEQ and ZF-TEQ are the same (cf. Equation (2.10)).

2.3.2 MMSE Frequency Domain Equalizer

Suppose $\mathbf{u}$ has identical and independent distributed (i.i.d.) elements each with zero mean and variance σ_u^2, the frequency domain scalar MSE to estimate $u_F(k)$ is defined by

$$\begin{aligned}\psi(k) &= E[|u_F(k)-\hat{u}_F(k)|^2] \\ &= E[|u_F(k)|^2]+E[|r_F(k)|^2]|x(k)|^2 \\ &\quad -2\operatorname{Re}\{x^*(k)E[r_F(k)u_F^*(k)]\}, \quad k = 0,\cdots,N-1\end{aligned} \tag{2.24}$$

where $E[|u_F(k)|^2]=\sigma_u^2$, $E[|r_F(k)|^2]=\sigma_u^2+\sigma_v^2$ and $E[r_F(k)u_F^*(k)]=g(k)\sigma_u^2$. And the corresponding scalar MMSE-FEQ is

$$\begin{aligned}x_{MMSE-FEQ}(k) &= \{E[|r_F(k)|^2]\}^{-1}\{E[r_F(k)u_F^*(k)]\} \\ &= \frac{g(k)}{|g(k)|^2+\sigma_v^2/\sigma_u^2}, \quad k = 0,\cdots,N\text{-}1\end{aligned} \tag{2.25}$$

Since $\mathbf{H}_r = \mathbf{F}_N^H\mathbf{G}\mathbf{F}_N$,

$$\begin{aligned}\mathbf{X}_{MMSE-FEQ} &= \left(\tfrac{\sigma_v^2}{\sigma_u^2}\mathbf{I}_N+\mathbf{G}\mathbf{G}^H\right)^{-1}\mathbf{G} \\ &= \left(\tfrac{\sigma_v^2}{\sigma_u^2}\mathbf{I}_N+\mathbf{F}_N\mathbf{H}_r\mathbf{H}_r^H\mathbf{F}_N^H\right)^{-1}\mathbf{F}_N\mathbf{H}_r\mathbf{F}_N^H \\ &= \mathbf{F}_N\left(\tfrac{\sigma_v^2}{\sigma_u^2}\mathbf{I}_N+\mathbf{H}_r\mathbf{H}_r^H\right)^{-1}\mathbf{H}_r\mathbf{F}_N^H\end{aligned} \tag{2.26}$$

and finally obtain

$$\mathbf{W}_{MMSE-FEQ} = \left(\tfrac{\sigma_v^2}{\sigma_u^2}\mathbf{I}_N+\mathbf{H}_r\mathbf{H}_r^H\right)^{-1}\mathbf{H}_r \tag{2.27}$$

Namely, MMSE-FEQ is also equivalent to MMSE-TEQ (cf. Equation (2.15)) if the assumption on $\mathbf{u}$ at the beginning is true.

2.3.3 Mean Square Error Performance

Similar to Equation (2.9), MSE for the whole data block in frequency domain can be defined by

$$\begin{aligned}\xi_F &= E\{\| \mathbf{u}_F - \hat{\mathbf{u}}_F \|^2\} \\ &= E\{\| \mathbf{u}_F - \mathbf{X}^H \mathbf{r}_F \|^2\} \\ &= \sum_{k=0}^{N-1} \psi(k)\end{aligned} \tag{2.28}$$

where $\psi(k)$ can be obtained according to ZF-FEQ and MMSE-FEQ respectively,

$$\psi_{ZF-FEQ}(k) = \sigma_v^2 / | g(k) |^2 \tag{2.29}$$

$$\psi_{MMSE-FEQ}(k) = \sigma_v^2 / (| g(k) |^2 + \sigma_v^2 / \sigma_u^2) \tag{2.30}$$

Then MSE can be represented by

$$\xi_{ZF-FEQ} = \sigma_v^2 tr\left[\left(\mathbf{G}\mathbf{G}^H\right)^{-1}\right] \tag{2.31}$$

$$\xi_{MMSE-FEQ} = \sigma_v^2 tr\left[\left(\frac{\sigma_v^2}{\sigma_u^2}\mathbf{I}_N + \mathbf{G}\mathbf{G}^H\right)^{-1}\right] \tag{2.32}$$

2.4 Equivalence of Time Domain Equalizer and Frequency Domain Equalizer

The equivalence of TEQ and FEQ based on the same optimal criterion (ZF or MMSE) is always held although only the special case is discussed when the scalar form of MMSE-FEQ exists. As to MSE performance (cf. Equations (2.9) and (2.28)), their equivalence can be easily seen from the property of matrix trace $tr(\mathbf{B}\mathbf{A}\mathbf{B}^{-1}) = tr(\mathbf{A})$.

However, MMSE-FEQ cannot be always expressed in such *scalar* form as Equation (2.25) unless the assumption presented in Section 2.3.2 on the statistics of $\mathbf{u}$ is held. Without scalar form, MMSE-FEQ will have no advantage over MMSE-TEQ in computational complexity sense.

Due to the equivalence of TED and FEQ in expressions and hence performances except the difference in complexity, they will not be distinguished in the sequel. And the assumption that $\mathbf{u}$ has i.i.d. elements with the same variance is used in what follows.

2.5 BER Performance for BPSK Block Transmission System

Suppose that the transmitted symbols are with the same power σ_u^2 and independently chosen from antipodal alphabet {+1, -1} with equal probabilities. Then the received data after a ZF equalizer are

$$\begin{aligned} \hat{\mathbf{u}}_{ZF} &= \mathbf{u} + \mathbf{H}_r^{-1}\mathbf{v} \\ &= \mathbf{u} + \mathbf{F}_N^H \mathbf{G}^{-1} \mathbf{F}_N \mathbf{v} \\ &\equiv \mathbf{u} + \hat{\mathbf{v}} \end{aligned} \tag{2.33}$$

or equivalently

$$\hat{u}_{ZF}(n) = u(n) + \hat{v}(n), \quad n = 0, \cdots, N-1 \tag{2.34}$$

where $\hat{v}(n) = \mathbf{e}_{N,n}^T(\mathbf{F}_N^H \mathbf{G}^{-1} \mathbf{F}_N \mathbf{v})$ and $\mathbf{e}_{N,n}$ is the nth column of the identity matrix $\mathbf{I}_N$. Obviously $\hat{v}(n)$ is still Gaussian distributed with zero mean but a variance conditioned on the channel $\sigma_v^2\left[\mathbf{e}_{N,n}^T\mathbf{F}_N^H(\mathbf{G}^H\mathbf{G})^{-1}\mathbf{F}_N\mathbf{e}_{N,n}\right]=\sigma_v^2\left[\mathbf{f}_{N,n}^T(\mathbf{G}^H\mathbf{G})^{-1}\mathbf{f}_{N,n}^*\right]=\frac{\sigma_v^2}{N}\sum_{k=0}^{N-1}\frac{1}{|g(k)|^2}$.

At the decision step, only the real part of the received data will be considered for the real-valued BPSK signals. Then

$$\mathrm{Re}\left(\hat{u}_{ZF}(n)\right)=u(n)+\mathrm{Re}\left(\hat{v}(n)\right),\quad n=0,\cdots,N-1 \tag{2.35}$$

Since $\mathrm{Re}[\hat{v}(n)]=[\hat{v}(n)+\hat{v}^*(n)]/2$, the variance of $\mathrm{Re}[\hat{v}(n)]$ can be derived by

$$\begin{aligned}\sigma_{\hat{v},re}^2(n)&=\frac{1}{4}E\left\{\left[\mathbf{e}_{N,n}^T(\mathbf{F}_N^H\mathbf{G}^{-1}\mathbf{F}_N\mathbf{v})+(\mathbf{v}^H\mathbf{F}_N^H\mathbf{G}^{-1}\mathbf{F}_N)\mathbf{e}_{N,n}\right]^2\right\}\\&=\frac{\sigma_v^2}{2N}\sum_{k=0}^{N-1}\frac{1}{|g(k)|^2}\end{aligned} \tag{2.36}$$

which implies the noise in each equalized sample has the same variance. Hence, the output SNR for the nth symbol is simply $SNR_{o,BPSK}(\mathbf{h})=\sigma_u^2/\sigma_{\hat{v},re}^2(n)$.

Then the averaged BER conditioned on $\mathbf{h}$ can be calculated through

$$P_{e,ZF}(\mathbf{h})=\mathbb{Q}\left[SNR_{o,BPSK}(\mathbf{h})\right] \tag{2.37}$$

where $\mathbb{Q}(x)=\frac{1}{\sqrt{2\pi}}\int_x^\infty e^{-t^2/2}dt$. If $\mathbf{h}$ is a stochastic channel with a probability density function (pdf) $f(\mathbf{h})$, the averaged BER will be

$$P_{e,ZF}=\int P_{e,ZF}(\mathbf{h})f(\mathbf{h})d\mathbf{h} \tag{2.38}$$

However, it is difficult to derive the closed-form BER for MMSE equalizer.

2.6 Simulation Results

Simulations have been performed for a block transmission system, where L=7 and each data block contains N=400 symbols. During the simulation, 100 data blocks are used. Variable input SNR is done through changing the noise variance while fixing the amplitude of transmitted symbols, since the MSE performance of ZF equalizer does not depend on signal power (cf. Equations (2.16) and (2.31)).

2.6.1 Deterministic Channel

Given a deterministic FIR channel [2] by

$$h(l) = \begin{cases} 0, & l = 0 \\ 0.5 + 0.5\cos[2\pi(l-1)/W], & l = 1,\cdots,L \end{cases} \tag{2.39}$$

where the parameter W controls the eigen spread χ_h of the channel matrix $\mathbf{H}_r$. For example, W = 1.2 leads to an invertible $\mathbf{H}_r$ with χ_h = 14.5.

In Figure 2.2, the symbol MSE is adopted, instead of MSE for the whole data block defined in Equation (2.9). The simulated results match the analytical results very well. ZF equalizer will approach to MMSE equalizer with increasing input SNR, since the higher input SNR, the less effect the noise has on the performance of the equalizer (cf. Equation (2.27)).

In Figure 2.3, simulated BER of ZF equalizer matches very well to the analytical result given by Equation (2.37). It has the same trend as the analitical MSE with increasing input SNR. Without surprise, MMSE equalizer results in a better BER than ZF equalizer because it balances the influence from ISI and additive noise.

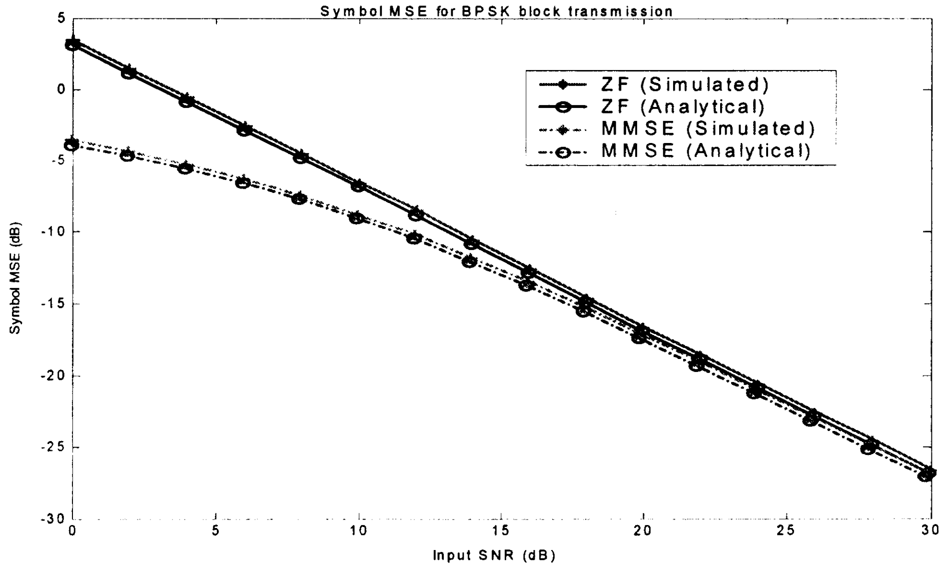

Figure 2.2 Symbol MSE given a deterministic channel for BPSK block transmission.

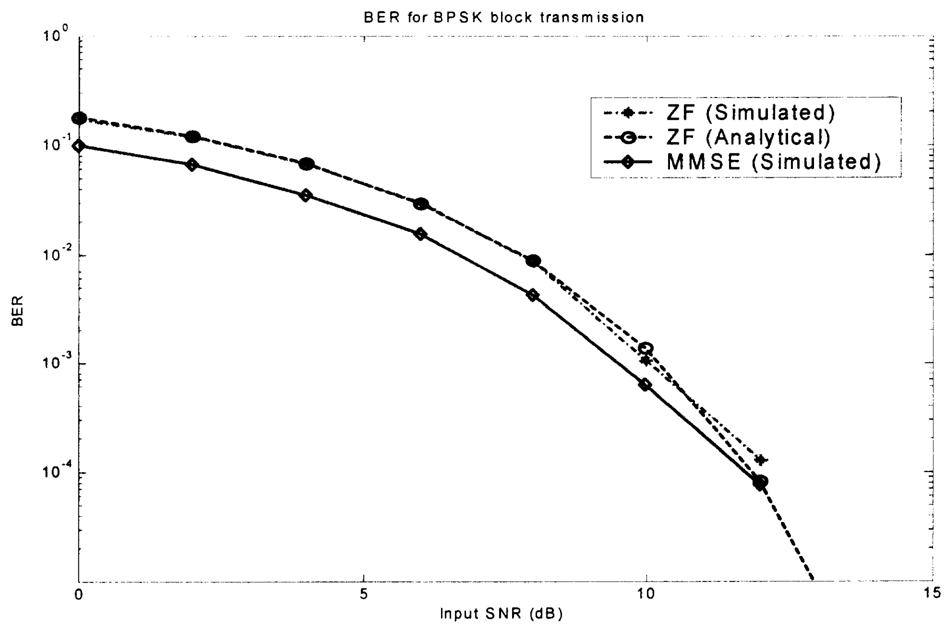

Figure 2.3 BER given a deterministic channel for BPSK block transmission.

2.6.2 Rayleigh Fading Channel

In the sequel, Rayleigh fading channel with two types of power decaying profiles (PDP) are considered: one with equally PDP (EQ-PDP) and the other with exponentially PDP (EXP-PDP). $\varphi^2(l)$ is assumed to be the average fading power of the lth delay bin and normalized as $\sum_{l=0}^{L}\varphi^2(l)=1$. Then

$$\text{EQ-PDP:} \quad \varphi^2(l)=1/(L+1), \quad l=0,\cdots,L \tag{2.40}$$

$$\text{EXP-PDP:} \quad \varphi^2(l)=\varphi^2(0)e^{-l/(L+1)}, \quad l=0,\cdots,L \tag{2.41}$$

where $\varphi^2(0)=1\Big/\left(\sum_{l=0}^{L}e^{-l/(L+1)}\right)$ for EXP-PDP.

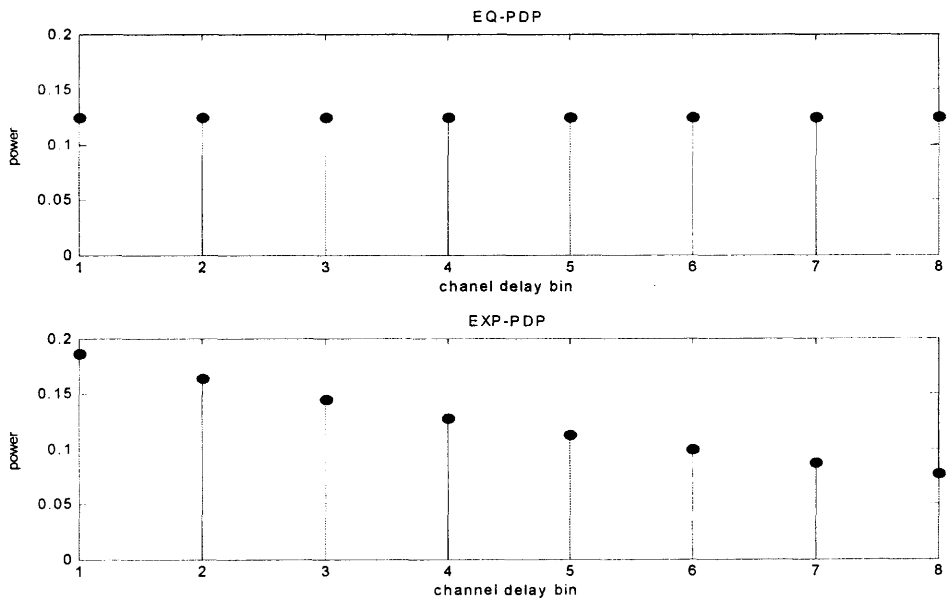

Figure 2.4 Normalized equally PDP and exponentially PDP with L = 7.

The channel gain for the lth delay bin can be obtained via the well-known AR model [3]:

$$h_{i+m}(l) = \alpha_m(l)\, h_i(l) + \eta_{i+m}(l), \quad l = 0, \cdots, L \tag{2.42}$$

where $h_i(l)$ subject to Jakes fading, stands for the complex channel gain of the lth delay bin in the ith frame and its variance is denoted by $\sigma^2_{h(l)}$. $\eta_{i+m}(l)$ is an independent complex Gaussian distributed random variable with zero mean and variance $\sigma^2_{\eta(l)}$ (note that $\sigma^2_{\eta(l)} + \sigma^2_{h(l)} = \varphi^2(l)$). The autocorrelation of the lth delay bin is defined by $\alpha_m(l) = E[h_i(l)h^*_{i+m}(l)] = J_0(2\pi m f_d T_f)$, where f_d is Doppler frequency, T_f is frame period and $J(\bullet)$ is the zeroth-order Bessel function of the first kind.

A mobile environment is considered where the vehicle speeds are 68 and 136 miles/h, corresponding to 30 and 60m/s. Given the carrier frequency $f_{ca} = 2\text{GHz}$ and symbol rate $f_s = 1.024\text{M}$, it comes up with the corresponding Doppler frequencies: 200Hz and 400Hz. And the channel coherence time is approximately $\tau = 0.5/f_d = 2.5\text{ms and } 1.25\text{ms}$ [4], resulting in the maximal number of the symbols per frame $f_s\tau = 2560 \text{ and } 1280$ respectively without suffering channel's time-variation. Therefore the selection on $N_f = N + N_c = 408$ can satisfy the block fading channel requirement.

Note that some realizations of a stochastic channel $\mathbf{h}$, the channel matrix $\mathbf{H}_r$ may be singular, in which case the symbols cannot be recovered using ZF equalizer. Therefore only the symbol MSE performance of MMSE equalizer is shown in Figure 2.5, where higher Doppler frequency leads to a little bit higher MSE when input SNR is high.

For the BER performance shown in Figure 2.6, ZF equalizer cannot recover the symbols well as mentioned before. This is indicated by the high error floors in both sub-figures. And similar to the symbol MSE performance, Doppler frequency will affect BER more in high input SNR. And BER performance in the EXP-PDP Rayleigh fading channel is worse than EQ-PDP case.

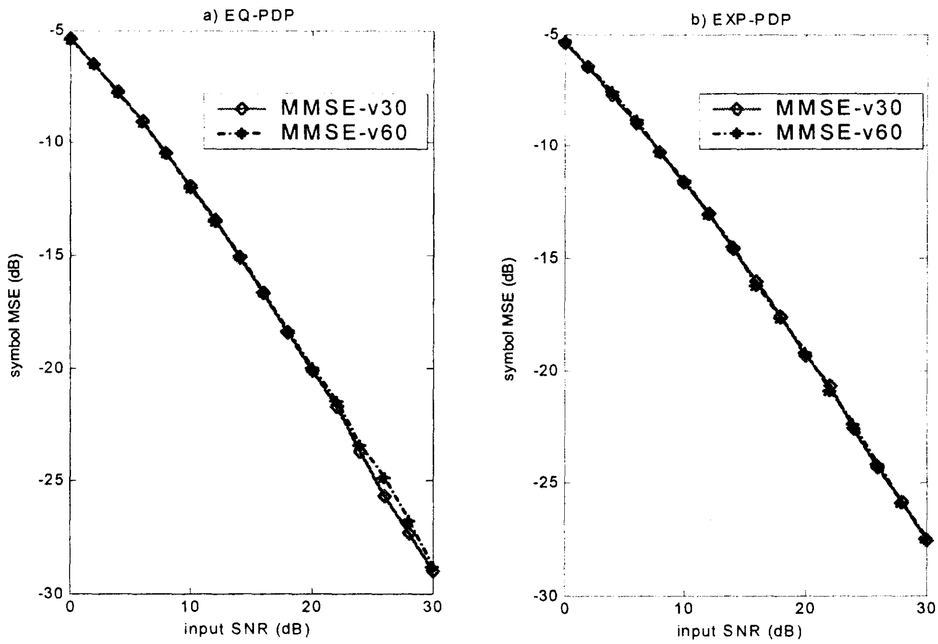

Figure 2.5 Symbol MSE of MMSE equalizer in Rayleigh fading channels for BPSK block transmission.

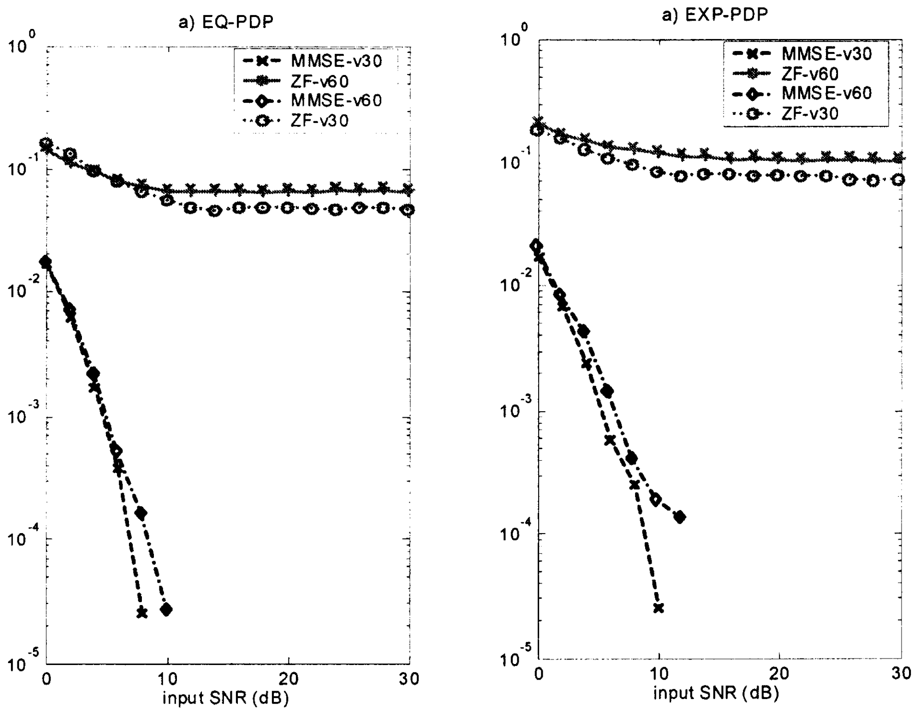

Figure 2.6 BER of ZF and MMSE equalizers in Rayleigh fading channels for BPSK block transmission.

CHAPTER 3

CYCLIC PREFIX ASSISTED CDMA SYSTEM

The CP-CDMA [1] was proposed to simplify the downlink receiver design in DS-CDMA system. Its advantages include 1) low complexity block equalization in frequency domain; 2) single user detection method can be used due to the usage of orthogonal spreading codes.

In this chapter, a low complexity frequency domain joint receiver is proposed. It consists of block equalization, de-spread and data detection. With a proper approximation on the statistics of the transmitted data, a scalar MMSE frequency domain equalizer will be derived.

3.1 System Structure

Figure 3.1 shows the structure of CP-CDMA system, where the receiver outputs the ith frame data of user 1, i.e., the desired user.

The notation in Figure 3.1 has the same meaning as that in Chapter 2. Additionally, the frame structure for CP-CDMA system is the same as in Figure 2.1 except that users' data block $\mathbf{u}(i)$ has special structure due to spreading. Assume that each block duration include B symbol intervals. $\mathbf{u}(i)=[\mathbf{u}^T(i,0),\cdots,\mathbf{u}^T(i,B-1)]^T$, where $\mathbf{u}(i,b)$ consists of the composite chip-rate signals within the bth symbol interval of the ith frame. That is,

$$\mathbf{u}(i,b) = \mathbf{SAd}(i,b) \tag{3.1}$$

where $\mathbf{S} = [\mathbf{s}_1, \cdots, \mathbf{s}_Q]$, $\mathbf{A} = diag(A_1, \cdots, A_Q)$ and $\mathbf{d}(i,b) = [d_1(i,b), \cdots, d_Q(i,b)]^T$. $\mathbf{s}_q$, A_q and $d_q(i,b)$ respectively represent the normalized orthogonal spreading code, amplitude and bth symbol for user q in the ith frame. Here, BPSK constellation is used, i.e., $d_q(i,b)$ is chosen from {+1, -1} with equal probabilities and independent of q, i and b. Therefore $N = BM$ and each chip is namely a sample described in Chapter 2.

The users' data can be rewritten as

$$\mathbf{u}(i) = \tilde{\mathbf{S}}\tilde{\mathbf{d}}(i) \tag{3.2}$$

where $\tilde{\mathbf{d}}(i) = \{[\mathbf{Ad}(i,0)]^T, \cdots, [\mathbf{Ad}(i,B-1)]^T\}^T$ and $\tilde{\mathbf{S}} = (\mathbf{I}_B \otimes \mathbf{S}) \in \mathbb{R}^{N \times BK}$ with $\otimes$ denoting the Kronecker product.

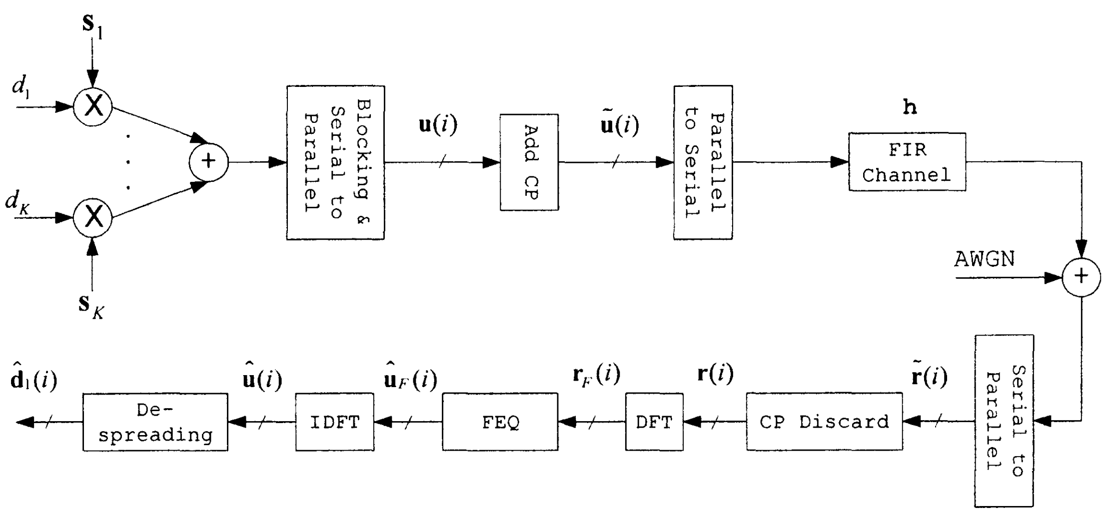

Figure 3.1 Block diagram of the CP-CDMA system.

3.2 Proposed Frequency Domain Joint Receiver

Exactly following the idea of cyclic prefix assisted block transmission in Chapter 2, the block equalization can be simplified in frequency domain. It must be emphasized that the following derivation related to FEQ is based on a basic assumption that FEQ matrix $\mathbf{W}_F$ can be eigen-decomposed by a DFT matrix, i.e., the scalar FEQ exists. In fact, such assumption is not held in CP-CDMA system if MMSE-FEQ is used. In the sequel, two steps are used to derive the joint receiver: 1) the assumption on the existence of the scalar FEQ is held for the equalization purpose; 2) then a reasonable approximation for the MMSE-FEQ is made in such block transmission application.

If the frame index is ignored without loss of generality, the estimate of whole composite users' data block can be obtained through an FEQ matrix $\mathbf{W}_{FEQ}$ such that

$$\hat{\mathbf{u}} = \mathbf{W}_{FEQ}^H \mathbf{r} \tag{3.3}$$

After de-spreading $\hat{\mathbf{u}}$ with the signature $\mathbf{s}_1$ for user 1, all the B estimated symbols for user 1 within a block are

$$\tilde{\mathbf{d}}_1 = \tilde{\mathbf{S}}_1^H \hat{\mathbf{u}} \tag{3.4}$$

where $\tilde{\mathbf{S}}_1 = (\mathbf{I}_B \otimes \mathbf{s}_1) \in \mathbb{R}^{N \times B}$. In fact, Equation (3.4) can be further simplified if the FEQ characteristics are considered, i.e.,

$$\tilde{\mathbf{d}}_1 = \tilde{\mathbf{S}}_{1,F}^H \left(\mathbf{X}^H \mathbf{r}_F \right) \tag{3.5}$$

where $\tilde{\mathbf{S}}_{1,F} = \mathbf{F}_N \tilde{\mathbf{S}}_1$ and $\mathbf{X}$ is a diagonal matrix defined in Equation (2.20). Since $\mathbf{s}_1$ is known at the receiver of user 1, $\tilde{\mathbf{S}}_{1,F}$ can be calculated offline in advance and stored at the receiver of user 1. Finally, the decision rule based on $\tilde{\mathbf{d}}_1$ is

$$\hat{\mathbf{d}}_1 = sign\left\{\mathrm{Re}(\tilde{\mathbf{d}}_1)\right\} \tag{3.6}$$

Remark: it can be observed from Equations (3.5) and (3.6) that the equalization, de-spread and detection can be done *jointly* in frequency domain, therefore the IDFT block in Figure 3.1 is not needed. The joint receiver structure can be represented by Figure 3.2.

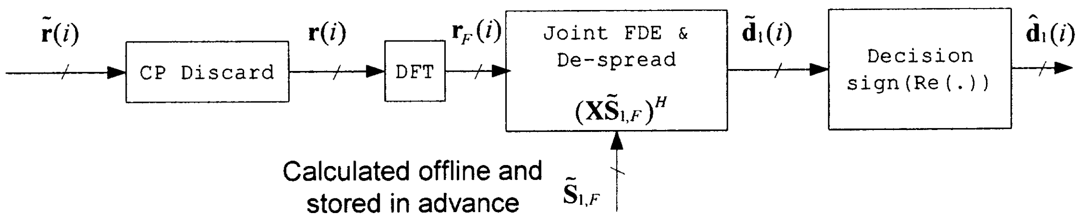

Figure 3.2 Proposed frequency domain joint receiver.

3.3 Performance of the Proposed Receiver

The performance of the proposed joint receiver will be discussed based on ZF-FEQ and MMSE-FEQ, respectively. From Equations (3.2), (3.3) and (3.4), $\tilde{\mathbf{d}}_1$ can be rewritten as

$$\begin{aligned}\tilde{\mathbf{d}}_1 &= \tilde{\mathbf{S}}_1^H \mathbf{W}_{FEQ}^H \mathbf{r} \\ &= \tilde{\mathbf{S}}_1^H \mathbf{W}_{FEQ}^H (\mathbf{H}_r \tilde{\mathbf{S}} \tilde{\mathbf{d}} + \mathbf{v}) \\ &= \tilde{\mathbf{S}}_1^H \mathbf{W}_{FEQ}^H \mathbf{H}_r \tilde{\mathbf{S}} \tilde{\mathbf{d}} + \tilde{\mathbf{S}}_1^H \mathbf{W}_{FEQ}^H \mathbf{v}\end{aligned} \tag{3.7}$$

where Equations (2.6) and (3.2) are directly applied.

3.3.1 Joint Receiver Based on Zero-Forcing Equalizer

If the ZF-FDE is applied, i.e., $\mathbf{W}_{ZF-FEQ}^{H} = \mathbf{H}_r^{-1}$, Equation (3.7) will be

$$\begin{aligned}\tilde{\mathbf{d}}_{1,ZF} &= \tilde{\mathbf{S}}_1^H \tilde{\mathbf{S}}\tilde{\mathbf{d}} + \tilde{\mathbf{S}}_1^H \mathbf{H}_r^{-1}\mathbf{v} \\ &= A_1\mathbf{d}_1 + \tilde{\mathbf{S}}_1^H \mathbf{H}_r^{-1}\mathbf{v} \\ &= A_1\mathbf{d}_1 + \tilde{\mathbf{v}}\end{aligned} \tag{3.8}$$

where MAI has been completely cancelled. Then the bth element of $\tilde{\mathbf{d}}_{1,ZF}$ is

$$\begin{aligned}\tilde{d}_{1,ZF}(b) &= \mathbf{e}_{B,b}^T\left(\tilde{\mathbf{S}}_1^H \tilde{\mathbf{S}}\tilde{\mathbf{d}} + \tilde{\mathbf{v}}\right) \\ &= \mathbf{e}_{B,b}^T\left(A_1\mathbf{d}_1 + \tilde{\mathbf{v}}\right) \\ &= A_1 d_1(b) + \tilde{v}(b), \quad b = 0,\cdots,B-1\end{aligned} \tag{3.9}$$

where $\tilde{v}(b) = \mathbf{e}_{B,b}^T \tilde{\mathbf{S}}_1^H \mathbf{H}_r^{-1}\mathbf{v} = \mathbf{e}_{B,b}^T \tilde{\mathbf{S}}_1^H \mathbf{F}_N^H \mathbf{G}^{-1}\mathbf{F}_N\mathbf{v}$ and $\mathbf{e}_{B,b}$ is the bth column of $\mathbf{I}_B$. $\tilde{v}(b)$ is still complex Gaussian distributed random variable with zero mean and a variance $\sigma_{\tilde{v}}^2(b,\mathbf{h}) \equiv \sigma_v^2\left[\mathbf{e}_{B,b}^T \tilde{\mathbf{S}}_1^H \mathbf{F}_N^H (\mathbf{G}^H\mathbf{G})^{-1}\mathbf{F}_N \tilde{\mathbf{S}}_1 \mathbf{e}_{B,b}\right]$ conditioned on $\mathbf{h}$.

Hence the averaged BER conditioned on $\mathbf{h}$ can be directly expressed by

$$P_{e,ZF-CDMA}(\mathbf{h}) = \frac{1}{B}\sum_{b=0}^{B-1} Q\left(\frac{\sqrt{2}A_1}{\sigma_{\tilde{v}}(b,\mathbf{h})}\right) \tag{3.10}$$

Figure 3.3 shows the BER performance of the proposed joint receiver for CP-CDMA based on ZF equalizer. The fixed channel is known and chosen from Equation (2.39) with a length $L+1 = 8$ taps normalized to the chip duration. Additionally, $W = 50.9$

is chosen, which corresponds to $\chi_h = 128.7$. As a result, the existence of $\mathbf{H}_r$ inverse is still guaranteed.

The simulation setup is listed as follows: Walsh codes with length $M = 16$, $B = 31$ information bits per frame and equal symbol power for each user. The simulated result matches the analytical one very well when the number of active users is $Q = 16$. For different system loadings, MAI does not influence the BER performance in theory due to the selection of orthogonal spreading codes.

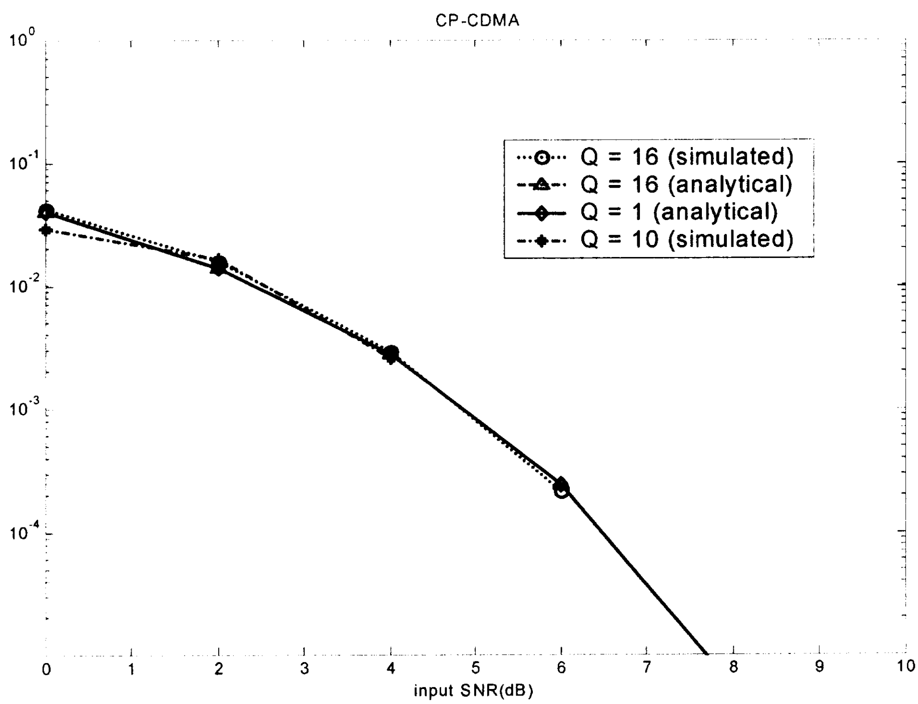

Figure 3.3 BER of the proposed joint receiver based on ZF equalizer given a deterministic channel for CP-CDMA system.

3.3.2 Joint Receiver Based on MMSE Equalizer

The MMSE equalizer for CP-CDMA system can be obtained similar to Equation (2.15), where

$$\mathbf{R}_u = \mathbf{I}_B \otimes (\mathbf{S}\mathbf{A}^2\mathbf{S}^H) \tag{3.11}$$

Obviously, $\mathbf{R}_u$ is not diagonal matrix, meaning that the scalar FEQ cannot be obtained!

However, an approximation [5] can be applied provided the assumption that all the spreading codes are unitary and all users' have the same amplitude, say A. In fact, Hermitian matrix $\mathbf{R}_u$ has band and block structure with all the diagonal elements equal to A^2Q/M and all other $Q-1$ diagonals not equal to but smaller than A^2Q/M. For a large block number B, $\mathbf{R}_u$ is a *sparse* matrix which can be approximated as $\mathbf{R}_u = \sigma_u^2 \mathbf{I}_{N\times N}$, where $\sigma_u^2 = A^2Q/M$. In fact, such approximation is better for a larger Q because the elements along all other $Q-1$ diagonals will be small due to the superposition of different orthogonal spreading codes. And this will be also observed in the following simulation results.

Consequently, the MMSE-FEQ can be achieved as

$$\widetilde{\mathbf{W}}_{MMSE-FEQ} = \left(\frac{\sigma_v^2}{\sigma_u^2} \mathbf{I}_N + \mathbf{H}_r \mathbf{H}_r^H \right)^{-1} \mathbf{H}_r \tag{3.12}$$

which has the same form as Equation (2.27). Therefore its scalar MMSE-FEQ can be achieved in the same way as Chapter 2. The subsequent de-spread and decision procedures are similarly based on Equations (3.6) and (3.7).

Figure 3.4 shows the simulated BER results for the joint receiver based on MMSE equalizer in Rayleigh fading channels. Here the vehicle speed is chosen as 136miles/h, namely 60m/s. To test the validity of the aforementioned approximation, the benchmark based on MUD, in which the true data statistics are given, is used. And the lines named by "approximated statistics" stands for the proposed joint receiver, which is based on the approximated statistics.

It says that such approximation is efficient for different system loadings and PDP of Rayliegh fading channels. Obviously, the approximation for $Q = 16$ is much better than $Q = 10$. And again, the BER performance of our proposed receiver is not much influenced by different system loadings if the orthogonal spreading codes are used.

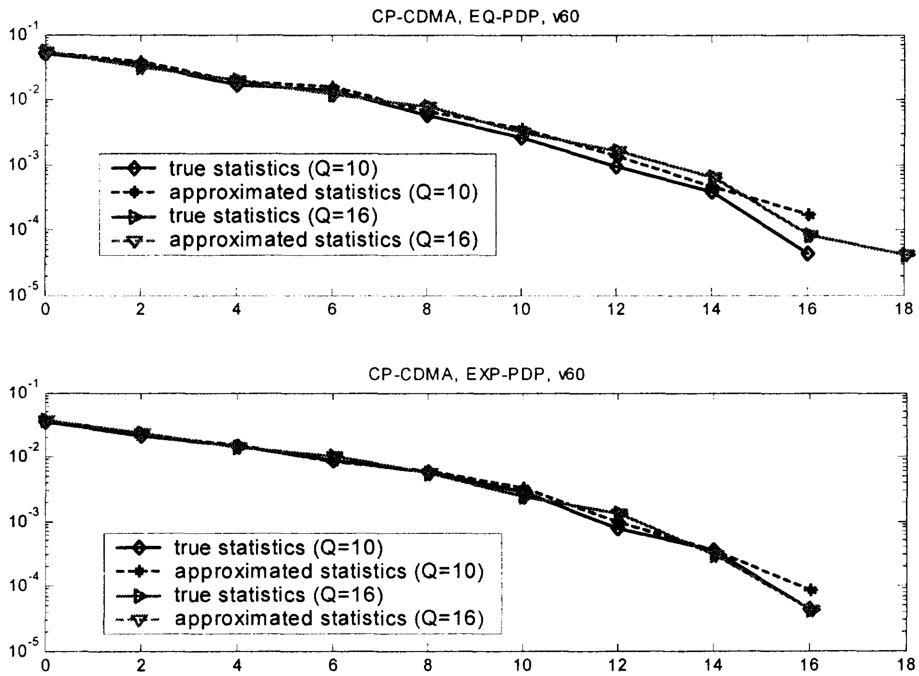

Figure 3.4 BER of the joint receiver based on MMSE equalizer in Rayleigh fading channels for CP-CDMA system.

CHAPTER 4

TRANING BASED CHANNEL ESTIMATION FOR BLOCK TRANSMISSION

The channel estimation algorithms described in this chapter make use of training sequences. And the data independent channel estimation methods will be studied, i.e., no users' data are involved during channel estimation.

A low complexity channel estimation method is proposed in this chapter. Then its performance is studied in a comparative way with the conventional method. At last, its applications to the BPSK block transmission system and the CP-CDMA system are explored.

4.1 Conventional Method

4.1.1 Frame Structure

In the conventional scheme, the training sequence (TS) is inserted between the consecutive data frames [1]. The frame structure is shown in Figure 4.1, where $\mathbf{p} = [p(0), \cdots, p(N_p - 1)]^T$ denotes the known TS. Throughout, the FIR channel is assumed to be invariant within the training period and the frame duration.

Within each training period, the received samples only affected by TS are

$$y(n) = \sum_{l=0}^{L} h(l) p(n-l) + v(n), \quad n = L, \cdots, N_p - 1 \tag{4.1}$$

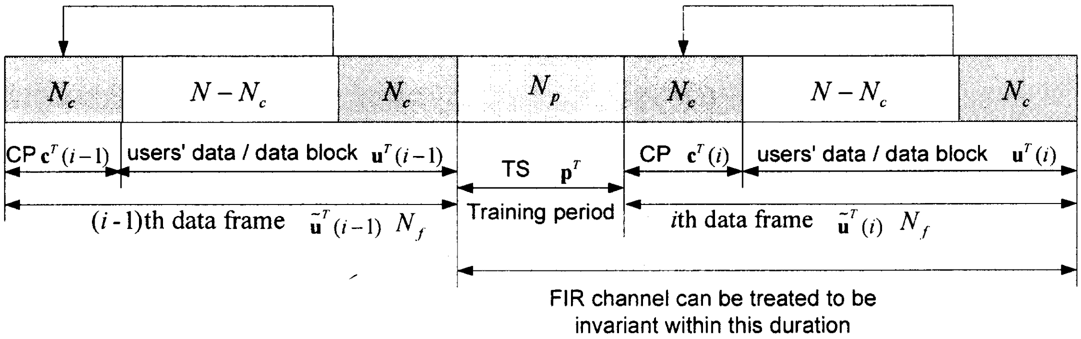

Figure 4.1 Frame structure of the conventional channel estimation method.

And the simpler matrix form is

$$\mathbf{y} = \mathbf{P}\mathbf{h} + \mathbf{v} \tag{4.2}$$

where $\mathbf{y} = [y(L), \cdots, y(N_p - 1)]^T$, and $\mathbf{v}$ denotes the AWGN vector with zero mean and covariance matrix $\sigma_v^2 \mathbf{I}_{N_p}$. $\mathbf{P} \in \mathbb{C}^{(N_p - L)\times(L+1)}$ is a *Toeplitz* matrix with the (*i*, *j*)th element $p(L+i-j)$, $i = 1, \cdots, N_p - L$ and $j = 1, \cdots, L+1$, i.e.

$$\mathbf{P} = \begin{bmatrix} p(L) & p(L-1) & \cdots & p(0) \\ p(L+1) & p(L) & \ddots & \vdots \\ \vdots & \ddots & \ddots & p(N_p - L) \\ p(N_p - 1) & \cdots & p(N_p - L) & p(N_p - L - 1) \end{bmatrix} \tag{4.3}$$

The channel total MSE (TMSE) in time domain can be defined by

$$\xi_{h,T} = E\{\| \mathbf{h} - \hat{\mathbf{h}} \|^2\} \tag{4.4}$$

where $\hat{\mathbf{h}}$ denotes the estimate of $\mathbf{h}$.

4.1.2 Time Domain Channel Estimation

Based on the observation model in Equation (4.2) and the white Gaussian assumption on the additive noise $\mathbf{v}$, the maximum-likelihood estimation (MLE) solution is the same as the least square solution, i.e.,

$$\hat{\mathbf{h}}_P = (\mathbf{P}^H\mathbf{P})^{-1}\mathbf{P}^H\mathbf{y} \tag{4.5}$$

A necessary condition for the channel to be identifiable is $N_p \geq 2L+1$, that is, $\mathbf{P}$ must have at least as many rows as columns. Such estimator results in an MSE

$$\begin{aligned}\xi_{h,T} &= \sigma_v^2 tr[(\mathbf{P}^H\mathbf{P})^{-1}] \\ &\equiv \sigma_v^2\Omega_p\end{aligned} \tag{4.6}$$

4.2 Proposed Method

Usually CP is used only to absorb the FIR channel, and discarded before equalization. However CP can be utilized in a more efficient way, leading to a simple frequency domain channel estimation algorithm.

4.2.1 Modified Frame Structure

Unlike the conventional method depicted in Section 4.1, TS is transformed to be CP, giving rise to a modified frame structure in Figure 4.2. N_c and N_u denote the lengths of TS (or CP) and the transmitted users' data $\mathbf{u}_u(i)$, respectively.

The ith frame can expressed by $\tilde{\mathbf{u}}(i) = [\mathbf{c}^T(i), \mathbf{u}^T(i)]^T = [\mathbf{c}^T(i), \mathbf{u}_u^T(i), \mathbf{c}^T(i)]^T$. Note that $\mathbf{u}_u(i)$ in this chapter has the same meaning as $\mathbf{u}(i)$ in Chapter 2, where the data block and users' data are identical. But now $\mathbf{u}(i)$ and $\mathbf{u}_u(i)$ are treated differently due to the introduction of TS in data block.

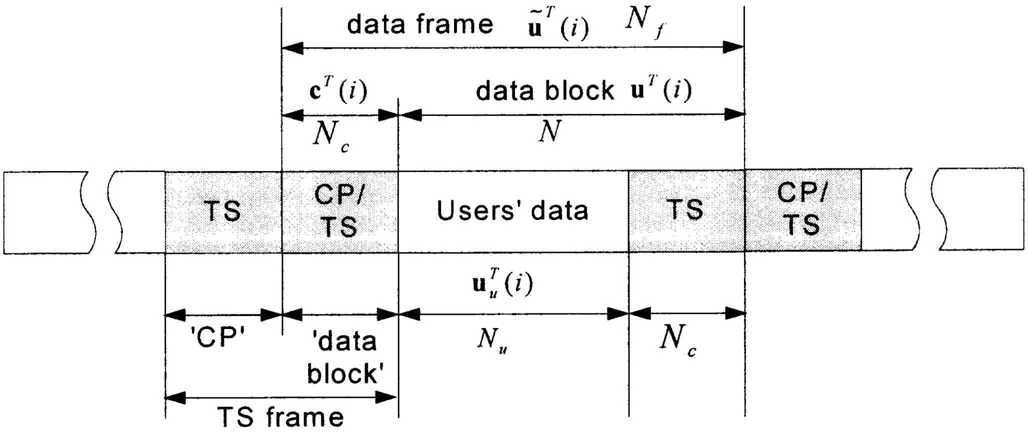

Figure 4.2 Frame structure of the proposed channel estimation method.

From the other angle, a TS frame can be virtually constructed: TS in the (i-1)th frame can be viewed as a "CP" for the "data block" in the ith frame given the identical TS for each frame. Obviously such virtual "data block" only consists of TS.

Following the same procedure as Section 2.1 and given $N_c = L+1$, the CP part in the ith received frame can be derived by

$$\begin{aligned}\mathbf{y}(i) &= \mathbf{T}_p\tilde{\mathbf{r}}(i) \\ &= \mathbf{T}_p\widetilde{\mathbf{H}}_0\mathbf{T}_{in}\mathbf{u}(i) + \mathbf{T}_p\widetilde{\mathbf{H}}_1\mathbf{T}_{in}\mathbf{u}(i-1) + \mathbf{T}_p\tilde{\mathbf{v}}(i)\end{aligned} \tag{4.7}$$

where $\mathbf{T}_p = [\mathbf{I}_{N_c}, \mathbf{0}_{N_c \times N}]$. Then $\mathbf{T}_p\widetilde{\mathbf{H}}_0\mathbf{T}_{in} = [\mathbf{0}_{N_c \times N_u}, \mathbf{H}_0]$ and $\mathbf{T}_p\widetilde{\mathbf{H}}_0\mathbf{T}_{in}\mathbf{u}(i) = \mathbf{H}_0\mathbf{c}(i)$ since $\mathbf{u}(i) = [\mathbf{u}_u^T(i), \mathbf{c}^T(i)]^T$, where

$$\mathbf{H}_0 = \begin{bmatrix} h(0) & 0 & \cdots & 0 \\ \vdots & \ddots & \ddots & \vdots \\ \vdots & \ddots & \ddots & 0 \\ h(L) & \cdots & \cdots & h(0) \end{bmatrix} \tag{4.8}$$

Similarly $\mathbf{T}_p \widetilde{\mathbf{H}}_1 \mathbf{T}_{in} \mathbf{u}(i-1) = \mathbf{H}_1 \mathbf{c}(i-1)$, where

$$\mathbf{H}_1 = \begin{bmatrix} 0 & h(1) & \cdots & h(L) \\ \vdots & \ddots & \ddots & \vdots \\ \vdots & \ddots & \ddots & h(1) \\ 0 & \cdots & \cdots & 0 \end{bmatrix} \tag{4.9}$$

Therefore

$$\mathbf{y}(i) = \mathbf{H}_0 \mathbf{c}(i) + \mathbf{H}_1 \mathbf{c}(i-1) + \mathbf{T}_p \tilde{\mathbf{v}}(i) \tag{4.10}$$

If the identical TS is denoted by $\mathbf{c}$ for each frame and the frame index is ignored without loss of generality, Equation (4.10) can be rewritten as

$$\begin{aligned} \mathbf{y} &= (\mathbf{H}_0 + \mathbf{H}_1)\mathbf{c} + \mathbf{T}_p \tilde{\mathbf{v}} \\ &= \mathbf{H}_c \mathbf{c} + \bar{\mathbf{v}} \end{aligned} \tag{4.11}$$

where $\mathbf{H}_c$ is a *circulant square* matrix with the first column specified by $\mathbf{h}$.

4.2.2 Frequency Domain Channel Estimation

Thanks to the circulant property of $\mathbf{H}_c$, a low-complexity frequency domain method can be applied to estimate $\mathbf{h}$ in a *scalar* fashion. Essentially, this is the same as the ZF-FEQ solution discussed in Chapter 2.

Define a unitary N_c-point DFT matrix $\mathbf{F}_{N_c} = [\mathbf{f}_{N_c,0},\ldots,\mathbf{f}_{N_c,N_c-1}]^H$, where $\mathbf{f}_{N_c,n}$ has the same form as $\mathbf{f}_{N,n}$ in Chapter 2 except replacing *N* with N_c. So, Equation (4.11) can be transformed into frequency domain as

$$\mathbf{y}_F = \mathbf{Z}\mathbf{c}_F + \bar{\mathbf{v}}_F \tag{4.12}$$

where $\mathbf{Z} = diag(\mathbf{z}) = \mathbf{F}_{N_c}\mathbf{H}_c\mathbf{F}_{N_c}^H$. $\mathbf{y}_F, \mathbf{c}_F, \bar{\mathbf{v}}_F$ and $\mathbf{z}$ respectively denote the N_c-point DFT vectors of $\mathbf{y}, \mathbf{c}, \bar{\mathbf{v}}$ and $\mathbf{h}$. Then the scalar form of Equation (4.12) is

$$y_F(k) = z(k)c_F(k) + \bar{v}_F(k), \qquad k = 0,\cdots,N_c-1 \tag{4.13}$$

Due to the Gaussian distributed property of $\bar{v}_F(k)$, the ML estimate of $z(k)$ can be easily obtained by

$$\hat{z}(k) = y_F(k)/c_F(k), \qquad k = 0,\cdots,N_c-1 \tag{4.14}$$

which always exists as long as $c_F(k) \neq 0, \forall k \in \{0,\cdots,N_c-1\}$. Finally the estimate of $\mathbf{h}$, denoted by $\hat{\mathbf{h}}_c$, can be obtained after performing N_c-point IDFT operation on $\hat{\mathbf{z}}$.

4.2.3 Mean Square Error Performance

Given white Gaussian distribution assumption on the additive noise, the ML solution for channel estimation has the same form as the ZF solution for equalization problem. Due to the equivalence of ZF-FEQ and ZF-TEQ shown in Chapter 2, a simpler TMSE form in frequency domain will be used to evaluate the proposed channel estimator.

From Equations (2.28), (2.29) and (4.4), the TMSE in frequency domain can be expressed by

$$\begin{aligned}\xi_{h,F} &= \sum_{k=0}^{N_c-1} \psi_{h,F}(k) \\ &\equiv \sigma_v^2 \Omega_c\end{aligned} \tag{4.15}$$

where $\psi_{h,F}(k) = \sigma_v^2 / |c_F(k)|^2$ and

$$\begin{aligned}\Omega_c &= \sum_{k=0}^{N_c-1} \left(1/|c_F(k)|^2\right) \\ &= tr[(\mathbf{C}_F^H \mathbf{C}_F)^{-1}] \\ &= tr[(\mathbf{C}^H \mathbf{C})^{-1}]\end{aligned} \tag{4.16}$$

where $\mathbf{C}_F = diag(\mathbf{c}_F)$ and $\mathbf{C}$ is a circulant square matrix with the first column specified by $\mathbf{c}$.

4.3 Optimal Training Sequence Design

Definition 4.1(Optimal training sequence): the training sequence is said to be optimal if no other counterparts under the same constraint can result in a smaller TMSE (or variance) $E\{\|\mathbf{h} - \hat{\mathbf{h}}\|^2\}$ based on the MLE method.

It is observed that the cost functions to design optimal TS are similar for two mentioned channel estimation methods (cf. Equations (4.6) and (4.16)): one is $tr[(\mathbf{P}^H\mathbf{P})^{-1}]$ and the other is $tr[(\mathbf{C}^H\mathbf{C})^{-1}]$. The sufficient and necessary condition to obtain optimal TS is the existence of $(\mathbf{P}^H\mathbf{P})^{-1}$ and $(\mathbf{C}^H\mathbf{C})^{-1}$. The optimal TS set may be different under different constraints even though the cost function is unchanged. Particularly, the optimal TS under two different constraints will be discussed.

4.3.1 Optimal Training Sequence Under Energy Constraint

Theorem 4.1: both channel estimators can achieve the same minimum TMSE under the same energy constraint $\mathbf{c}^H\mathbf{c} = \mathbf{p}^H\mathbf{p} = \lambda$, where $\lambda > 0$.

Before proving this theorem, a useful lemma in [7] should be introduced,

Lemma 4.1: Let a $n \times M$ matrix $\mathbf{B}$ be such that $tr(\mathbf{B}^H\mathbf{B}) \le \lambda M$ for some constraint $\lambda > 0$. Then, provided that the inverse exists, $tr[(\mathbf{B}^H\mathbf{B})^{-1}] \ge \lambda^{-1}M$, with equality if and only if $\mathbf{B}^H\mathbf{B} = \lambda\mathbf{I}_M$.

Theorem 4.2(Optimal TS for the conventional method):

1) $\mathbf{p}^H\mathbf{p} = \lambda$ implies $\xi_{h,T} \ge \sigma_v^2\lambda^{-1}(L+1)$ (cf. Equation (4.6)).

2) $\mathbf{p}$ is optimal if and only if $\mathbf{P}^H\mathbf{P} = \lambda\mathbf{I}_{L+1} = (\mathbf{p}^H\mathbf{p})\mathbf{I}_{L+1}$, in which case it reaches the lower bound $\xi_{h,T} \ge \sigma_v^2(\mathbf{p}^H\mathbf{p})^{-1}(L+1)$. A necessary condition for optimality is that $p(n) = 0$ for $n \le L$ and $n > N_p - L$.

Proof: Since $tr(\mathbf{P}^H\mathbf{P}) = \sum_{n=1}^{L} n\,|\,p(n-1)\,|^2 + \sum_{n=L+1}^{N_p-L}(L+1)\,|\,p(n-1)\,|^2 + \sum_{n=1}^{L} n\,|\,p(N_p-n)\,|^2$ and $tr(\mathbf{P}^H\mathbf{P}) \le \lambda(L+1)$, obviously with equality if and only if that $p(n) = 0$ for $n \le L$ and $n > N_p - L$, then 1) and 2) are proved directly from Lemma 4.1.

Theorem 4.3(Optimal TS for the proposed method):

1) $\xi_{h,T} \geq \sigma_v^2 \lambda^{-1}(L+1)$ (cf. Equation (4.15)) with the energy constraint $\mathbf{c}^H \mathbf{c} = \lambda$ if $\mathbf{P}$ is replaced by $\mathbf{C}$.

2) $\mathbf{c}$ is optimal if and only if $\mathbf{C}^H \mathbf{C} = \lambda \mathbf{I}_{N_c}$, in which case it reaches the lower bound $\xi_{h,T} \geq \sigma_v^2 (\mathbf{c}^H \mathbf{c})^{-1}(L+1)$.

Proof: Since $tr(\mathbf{C}^H \mathbf{C}) = (L+1)(\mathbf{c}^H \mathbf{c}) = (L+1)\lambda$, which always reaches the lower bound, then 1) and 2) are proved directly from Lemma 4.1.

From the two theorems, our claim is proved even though the proposed scheme has only nearly half overhead of the conventional method. The other advantage of the proposed method is that the search of optimal TS can be done in frequency domain, leading to much lower computational complexity. The comparison is listed in Table 4.1 to identify an unknown FIR channel of order L+1.

Suppose the TS for two methods are with the shortest lengths, i.e., $N_p = 2L+1$ and $N_c = L+1$. It can be found that the optimal TS are $\{\sqrt{\lambda}\delta(m-(L+1)), m = 0,\cdots,2L\}$ and $\{\sqrt{\lambda}\delta(m), m = 0,\cdots,L\}$, respectively for the conventional method and the proposed method. And the identical minimum TMSE is $(L+1)\sigma_v^2$. It is interesting to observe that optimal TS for two methods have a flat power spectrum, i.e. it excites all channel frequencies equally.

Table 4.1 Comparison of Channel Estimation Methods

	Conventional method	Proposed method
Overhead	$N_p \geq 2L+1$	$N_c \geq L+1$
Computational complexity	Inversion operation of an $N \times N$ matrix	2 N_c-point DFT and a one-step scalar division, usually $N_c \ll N$
Optimal TS Design	Minimize $\Omega_p = tr[(\mathbf{P}^H\mathbf{P})^{-1}]$	Minimize $\Omega_c = \sum_{k=0}^{N_c-1}\left(1/\lvert c_F(k)\rvert^2\right)$
TMSE	$\sigma_v^2\Omega_p$ (cf. Equation (4.6))	$\sigma_v^2\Omega_c$ (cf. Equation (4.16))
Common characteristics	1. Independence of users' data and the channel's statistics 2. Capability of identifying any FIR channel as long as the channel variation within each training period is negligible	

4.3.2 Optimal Training Sequence Under Antipodal Alphabet Constraint

For now, the same antipodal alphabet constraint is used to design optimal TS for both methods. Suppose $\mathbf{p} = A_0\mathbf{p}_0$ and $\mathbf{c} = A_0\mathbf{c}_0$, where A_0 is the envelope amplitude of training sequences. And the elements of $\mathbf{c}_0$ and $\mathbf{p}_0$ are chosen from the antipodal alphabet $\{+1,-1\}$. Hence, $\mathbf{c}_0^H\mathbf{c}_0 = N_c$ and $\mathbf{p}_0^H\mathbf{p}_0 = N_p$, meaning that they have different energy constraints.

1. Optimal Training Sequence for the Conventional Method

To simplify the design, a new cost function $\overline{\Omega}_p$ is introduced such that

$$\begin{aligned}\overline{\Omega}_p &= \Omega_p A_0^2 \\ &= tr[(\mathbf{P}_0^H \mathbf{P}_0)^{-1}]\end{aligned} \tag{4.17}$$

where $\mathbf{P} = A_0 \mathbf{P}_0$.

It is convenient to use eigen analysis method to explore the characteristics of optimal TS. Obviously $tr(\mathbf{P}_0^H \mathbf{P}_0) = \sum_{k=0}^{L} \lambda_k \equiv \beta$, where $\{\lambda_k, \quad k = 0, \cdots, L\}$ represent the eigenvalue set of $\mathbf{P}_0^H \mathbf{P}_0$. The Lagrange multiplier technique shows that $\overline{\Omega}_p = \sum_{k=0}^{L} \lambda_k^{-1} \geq (L+1)^2 / \beta$, with equality if and only if $\lambda_k = \beta/(L+1)$. Consequently $\beta = L+1$, implying $\{\lambda_k = 1, \quad k = 0, \cdots, L\}$ for optimality. Recalling the previous discussion, the minimum $\overline{\Omega}_p$ is 1 from the Theorem 4.2 if the energy constraint $\mathbf{p}_0^H \mathbf{p}_0 = N_p$ is applied.

Attention should be paid that there is *monotonical* relationship between the eigen spread of $\mathbf{P}_0^H \mathbf{P}_0$ and the value of $\overline{\Omega}_p$, i.e. the smaller eigen spread the smaller $\overline{\Omega}_p$. This is also equivalent to say that optimal TS with the minimal eigen spread (or minimal $\overline{\Omega}_p$) excites the channel frequencies as equally as possible.

2. Optimal Training Sequence for the Proposed Method

Similarly based on Equation (4.17), a new cost function $\overline{\Omega}_c = \Omega_c A_0^2$ can be used

$$\begin{aligned}\overline{\Omega}_c &= \sum_{k=0}^{N_c-1} 1/|c_{0,F}(k)|^2 \\ &= tr[(\mathbf{C}_{0,F}^H \mathbf{C}_{0,F})^{-1}] \\ &= tr[(\mathbf{C}_0^H \mathbf{C}_0)^{-1}]\end{aligned} \tag{4.18}$$

where $\mathbf{C}_{0,F} = diag(\mathbf{c}_{0,F})$ and $\mathbf{c}_{0,F}$ is the N_c-point DFT vector of $\mathbf{c}_0$. $\mathbf{C}_0$ is a circulant square matrix with the first column specified by $\mathbf{c}_0$.

Following the same derivation in Section 4.4.1 and considering the eigenvaule $\lambda_k = |c_{0,F}(k)|^2$ of $\mathbf{C}_{0,F}^H \mathbf{C}_{0,F}$ due to the diagonal property of $\mathbf{C}_{0,F}$, the objective is to minimize the eigen spread of $\mathbf{C}_{0,F}^H \mathbf{C}_{0,F}$ (or $\mathbf{C}_0^H \mathbf{C}_0$). This is equivalent to minimize the maximum-to-minimum ratio of $\{|c_{0,F}(k)|^2, k = 0,\cdots,N_c - 1\}$, to minimize $\overline{\Omega}_c$. Recalling the previous discussion, the minimum $\overline{\Omega}_c$ is 1 from Theorem 4.3 if the energy constraint $\mathbf{c}_0^H \mathbf{c}_0 = N_c$ is applied.

3. Comparison on Training Sequences

Given $A_c = 1$, $L = 7$ and $N_c = 8$, there are 32 optimal TS with minimum $\overline{\Omega}_c = 1.3333$ for the proposed method. However, there are only 4 optimal TS with minimal $\overline{\Omega}_p = 1.3$ for the conventional method. The optimal training sequences are shown in Table 4.2, where code index is defined as the decimal value corresponding to the binary code with "-1" replaced by "0".

Then it can be concluded that the optimal TS for both methods have almost the same TMSE performance provided the same antipodal alphabet constraint, but the proposed method has lower system overhead than the conventional method.

The other aspect on TS is the relation between its resulting TMSE and the eigen spread mentioned before. As to the TS for the conventional method, the following examples are listed in Table 4.3. However, as to the TS for the proposed method, there is a more convenient way.

Table 4.2 Optimal Training Sequences for $L = 7$

Code index of the optimal TS for the conventional and proposed methods	
Conventional method	Proposed method
2333, 9143, 23624, 30434	11, 13, 22, 26, 44, 47, 52, 61, 67, 79, 88, 94, 97, 104, 121, 122, 133, 134, 151, 158,161, 167, 176, 188, 194, 203, 208, 211, 229, 233, 242, 244

Table 4.3 Effect of Eigen Spread of $\mathbf{P}_0^H\mathbf{P}_0$ on TMSE Given the Code Length 15

Conventional method	Optimal TS	Code 835	Code 378	Code 85
Eigen spread of $\mathbf{P}_0^H\mathbf{P}_0$	4.1596	7.7634	21.6927	25.2741
$\overline{\Omega}_P$	1.3	1.5267	3.0	4.0

Due to the circulant property of $\mathbf{C}_0$, the eigenvalues of $\mathbf{C}_0^H\mathbf{C}_0$ are namely $\{|c_{0,F}(k)|^2, k = 0,\cdots,N_c - 1\}$, where $|c_{0,F}(k)|^2$ is the power at kth frequency bin. Therefore it can be easily found that the monotonical relation between TMSE and the eigen spread of $\mathbf{C}_{0,F}^H\mathbf{C}_{0,F}$ (or $\mathbf{C}_0^H\mathbf{C}_0$) in Figure 4.3. The other observation is that optimal TS for the proposed method have exactly same power profile in discrete frequency domain, where the power at the kth frequency bin is defined by $|c_{0,F}(k)|^2$ for TS $\mathbf{c}_0$.

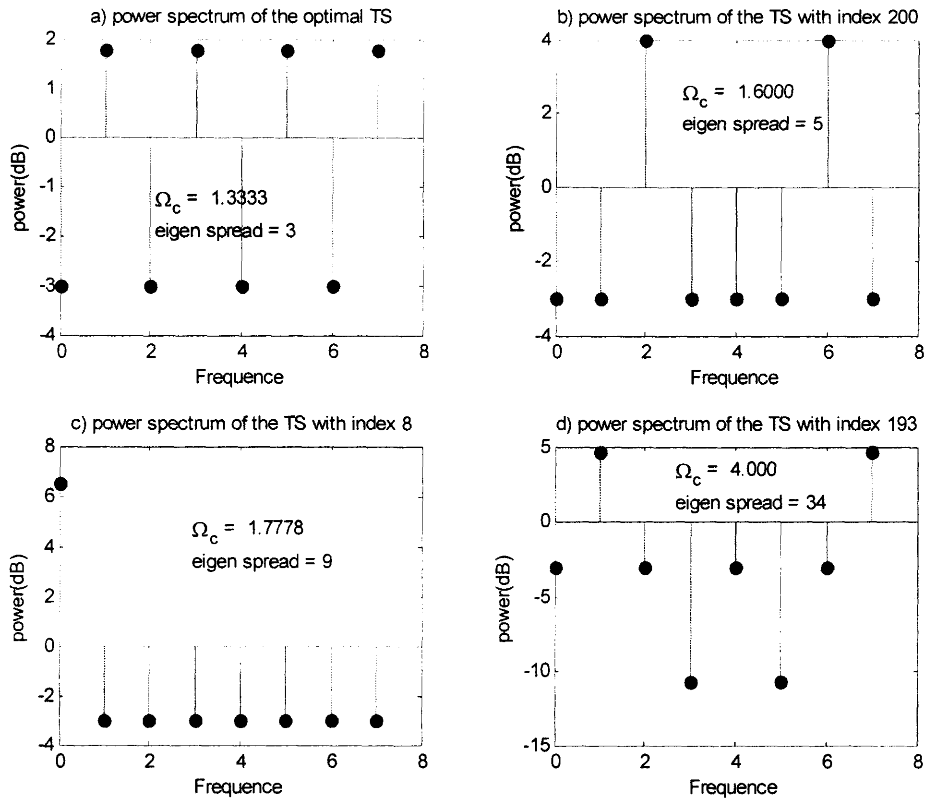

Figure 4.3 Discrete power spectrum of training sequences for the proposed method.

4.4 Application to BPSK Block Transmission System

Due to the insertion of TS in each frame for channel estimation, a slight modification should be made to detect BPSK symbols. BPSK symbols are assumed to be independent and with the same variance σ_u^2. Note that performing block equalization will be based on the estimated channel $\hat{\mathbf{h}}$, which equals to either $\hat{\mathbf{h}}_p$ for the conventional method or $\hat{\mathbf{h}}_c$ for the proposed method.

To demonstrate the influence of TS on signal detection, two types of interferences related to TS are defined: 1) *indirect TS interference*: introduced by TS through channel estimation error; 2) *direct TS interference*: introduced by TS if the CSI is known, i.e., no channel estimation error. If the conventional channel estimation method is used, only indirect TS interference is included in signal detection, thanks to the frame structure in Figure 4.1. Such scheme leads to the same signal detection procedure discussed in Chapters 2 and 3 except that circulant matrix $\mathbf{H}_r$ in equalizers is replaced by its estimate $\widehat{\mathbf{H}}_{r,p}$ constructed by $\hat{\mathbf{h}}_p$ in the same way as Equation (2.7).

However, the proposed channel estimation method gives rise to both indirect and direct TS interferences in signal detection because TS is also involved in the data block to be equalized. Based on the modified frame structure in Figure 4.2, $\mathbf{u} = [\mathbf{u}_u^T, \mathbf{c}^T]^T$. The estimate $\hat{\mathbf{u}}$ can be obtained through a block equalizer matrix $\widehat{\mathbf{W}}$ (cf. Equation (2.8)) based on the circulant square matrix $\widehat{\mathbf{H}}_{r,c}$ given $\hat{\mathbf{h}}_c$. For the ZF equalization, the block equalizer matrix has the same form as Equation (2.10) except using $\widehat{\mathbf{H}}_{r,c}$, namely,

$$\widehat{\mathbf{W}}_{ZF} = (\widehat{\mathbf{H}}_{r,c}^{-1})^H \tag{4.19}$$

Obviously, there will be no residual ISI in the equalized data if the channel is perfectly estimated, in which case TS has no influence on detection results. This means that TS influences the detection only through the channel estimation error, i.e. only indirect TS influence exists for the ZF equalizer.

However, for MMSE equalization, the situation is different. $\widehat{\mathbf{W}}_{MMSE}$ has the same from as Equation (2.15) except that

$$\mathbf{R}_u = \begin{bmatrix} \mathbf{R}_{uu} & \mathbf{0}_{N_u \times N_c} \\ \mathbf{0}_{N_c \times N_u} & \mathbf{R}_c \end{bmatrix} \tag{4.20}$$

where $\mathbf{R}_{uu} = E(\mathbf{u}_u \mathbf{u}_u^H) = \sigma_u^2 \mathbf{I}_{N_u}$, $\mathbf{R}_c = \mathbf{c}\mathbf{c}^H$ and $E(\mathbf{u}_u \mathbf{c}^H) = \mathbf{0}_{N_u \times N_c}$. Therefore the MMSE equalizer based on the proposed channel estimation method is given by

$$\widehat{\mathbf{W}}_{MMSE} = \left(\sigma_v^2 \mathbf{I}_N + \widehat{\mathbf{H}}_{r,c} \mathbf{R}_u \widehat{\mathbf{H}}_{r,c}^H\right)^{-1} \widehat{\mathbf{H}}_{r,c} \mathbf{R}_u \tag{4.21}$$

According to Equation (4.21), the interferences from TS are twofold: one is due to channel estimation error embedded in $\widehat{\mathbf{H}}_{r,c}$, i.e. indirect TS interference; the other is reflected in the autocorrelation matrix $\mathbf{R}_u$ (cf. Equation (4.20)), i.e., direct TS interference. From the other angle, ISI, including TS interference, always exists because of the scheme of MMSE criterion. The explicit influence of TS on the receiver performance is difficult to be obtained. In what follows, the performance will be explored through simulations.

Due to the introduction of non-diagonal matrix $\mathbf{R}_c$, the scalar FEQ form of $\widehat{\mathbf{W}}_{MMSE}$ cannot be achieved. However, still based on the same reason mentioned in Section 3.3.2 (the band, bock sparse structure $\mathbf{R}_u$ for a large N), $\mathbf{R}_u$ can be approximated by $\sigma_u^2 \mathbf{I}_N$ if $A_0^2 = \sigma_u^2$ is chosen. Then the MMSE equalizer matrix can be expressed by

$$\widetilde{\widehat{\mathbf{W}}}_{MMSE} = \left(\frac{\sigma_v^2}{\sigma_u^2} \mathbf{I}_N + \widehat{\mathbf{H}}_{r,c} \widehat{\mathbf{H}}_{r,c}^H\right)^{-1} \widehat{\mathbf{H}}_{r,c} \tag{4.22}$$

whose scalar MMSE-FEQ is similar to Equation (2.25). Finally, only the first N_u samples of $\hat{\mathbf{u}}$ are used to estimate $\mathbf{u}_u$, namely $\hat{\mathbf{u}}_u = \mathbf{T}_u \hat{\mathbf{u}}$ where $\mathbf{T}_u = [\mathbf{I}_{N_u}, \mathbf{0}_{N_u \times N_c}]$.

To demonstrate the performances associating to the input SNR, the amplitude of the transmitted symbols is fixed but the variance of additive noise is variable. Furthermore, the TS amplitude A_0 is set to be equal to the amplitude of BPSK symbols. In this case, input SNR is equal to the SNR of training sequences. Therefore they will treated the same in this section. This implies that the SNR of training sequence is changing according to the noise variance.

4.4.1 Deterministic Channel

In simulations, the same setup is used as Section 2.6.1 except that $W = 50.9$. The TMSE performances of both channel estimation methods are compared in Figure 4.4.

TMSE values of the selected TS, given $A_0 = 1$ and $\sigma_v^2 = 1$, have been given in Table 4.3 and Figure 4.4. It can be seen that optimal TS for each method has lower TMSE than the other non-optimal TS. And both methods lead to almost the same TMSE if their own optimal TS are chosen. Additionally, TMSE dose not relay on the characteristics of the FIR channel and signal alphabet, therefore the results in Figure 4.4 are also suitable for any FIR channels and any signal alphabet.

In Figures 4.5 and 4.6, the BER performances of both methods are compared. As expected, optimal TS lead to lower BER than any other non-optimal TS.

In Figure 4.7, the BER performances of both methods are further compared if their own optimal TS are used. It shows that both methods also have similar BER performance if the same kind of equalizer is used. For the detector based on MMSE-FEQ, the proposed approximation on the statistics is reasonable. The performance degradation due to the channel estimation error is also shown. And such error has more negative effect on ZF equalizer than MMSE equalizer if input SNR is high.

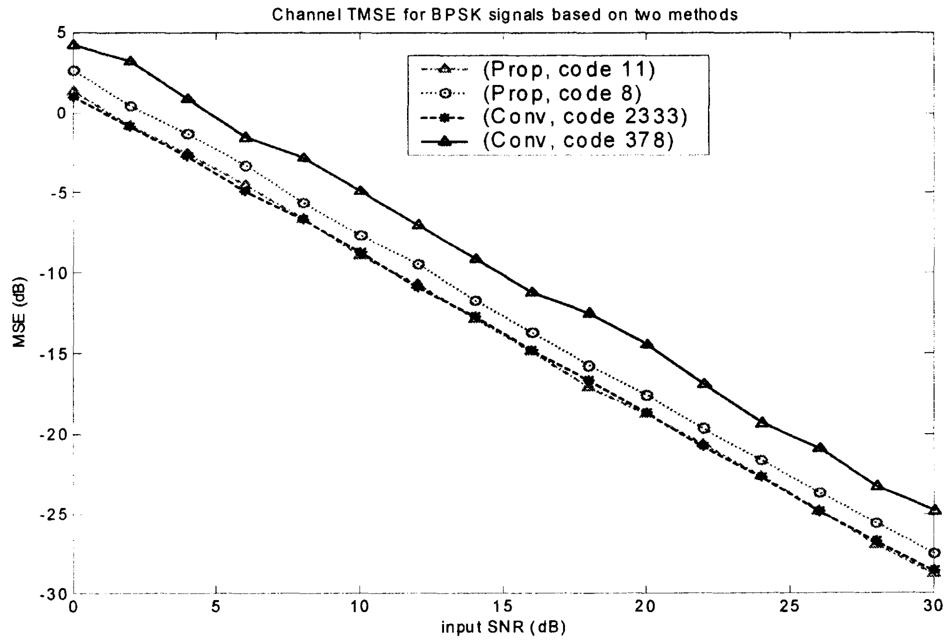

Figure 4.4 Channel TMSE of two methods given a deterministic channel (BPSK).

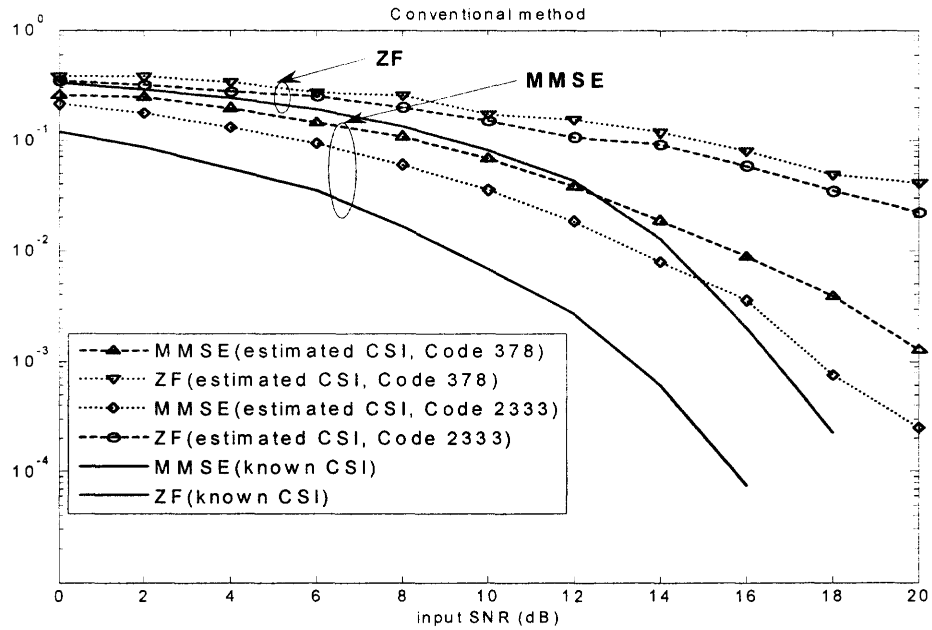

Figure 4.5 BER of the conventional method given a deterministic channel (BPSK).

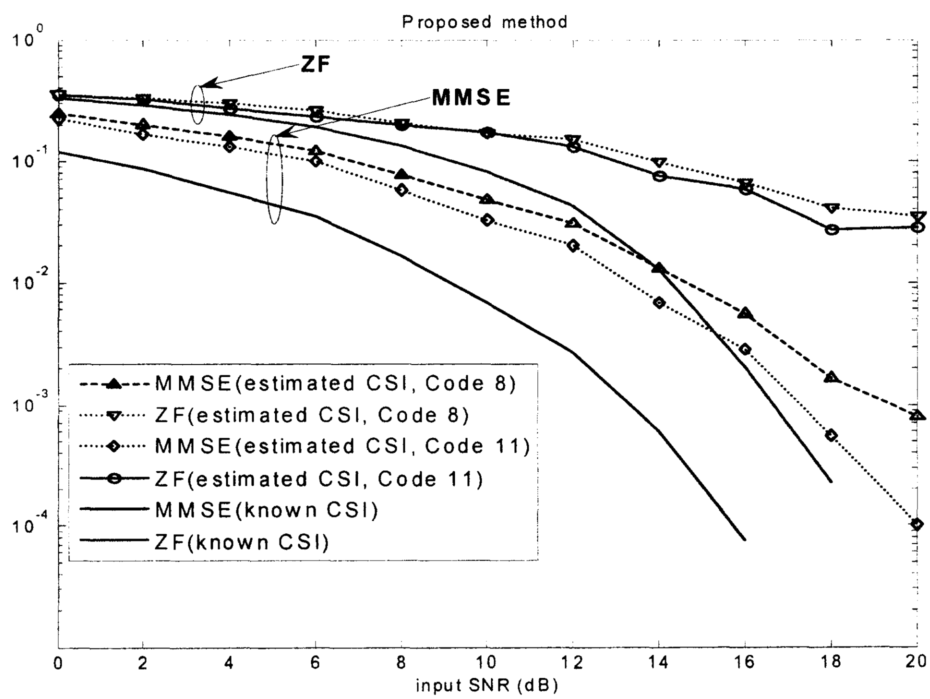

Figure 4.6 BER of the proposed method given a deterministic channel (BPSK).

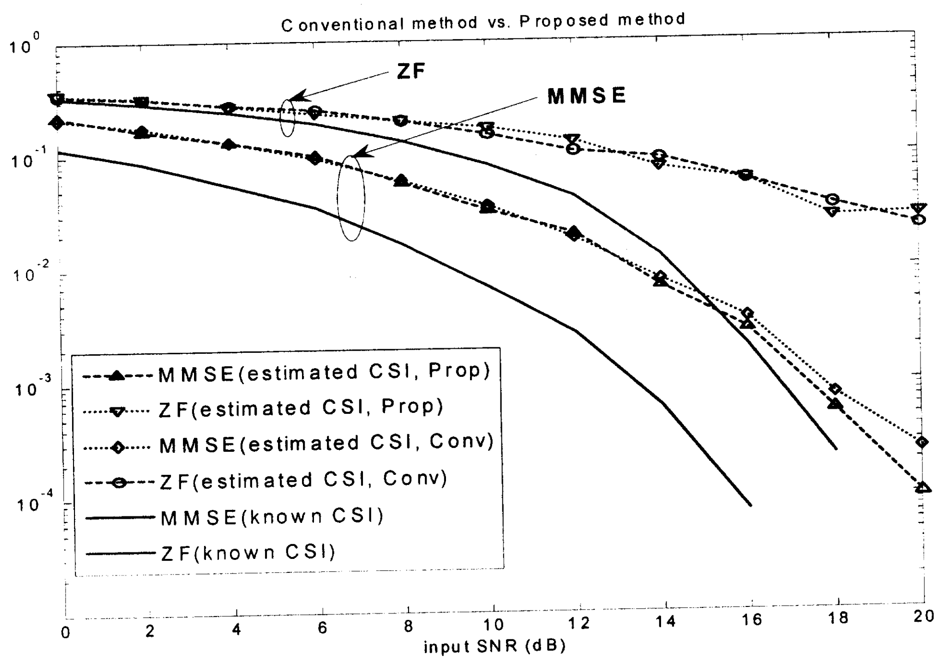

Figure 4.7 BER comparisons given a deterministic channel (BPSK).

4.4.2 Rayleigh Fading Channel

The same Rayleigh fading channel model as Chapter 2 is used. Still due to the restriction of ZF equalizer's capability to identify an FIR channel, only MMSE equalizer is considered. Figure 4.8 shows the BER performance of MMSE equalizer based on two mentioned channel estimation methods if their own optimal TS are chosen. The "Prop" and "Conv" denote the proposed method and the conventional method, respectively.

It can be observed that the BER difference between these two channel estimation methods is very small. Although Doppler frequency has not much effect on the performance when input SNR is low, but the PDP style influences the performance much. And the performance gap due to the channel estimation error is about 4dB.

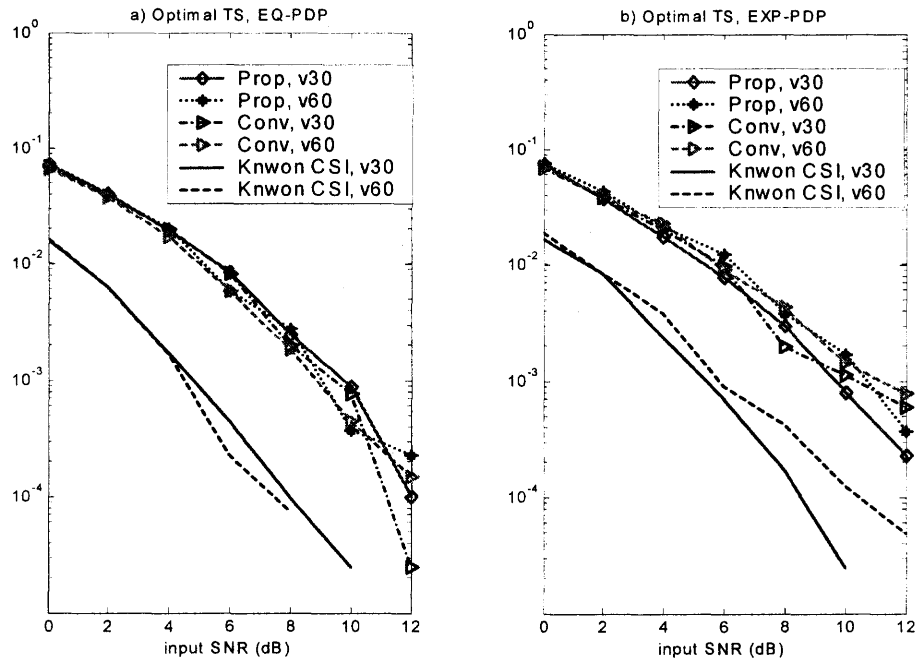

Figure 4.8 BER comparisons in Rayleigh fading channels (BPSK).

4.5 Application to CP-CDMA System

Following the similar steps in Section 4.4, the estimate of $\mathbf{u}_u$ can be obtained except that $\mathbf{u}_u = \tilde{\mathbf{S}}\tilde{\mathbf{d}}$ for CP-CDMA system (cf. Equation (3.1)). Note again that $\mathbf{u}_u$ is the same as $\mathbf{u}$ in Chapter 3. Additionally, if the conventional channel estimation method is applied, only the indirect TS interference is introduced (cf. Section 4.4).

For the proposed channel estimation method, the resulting ZF equalizer is still the same as Equation (4.19), which only introduces the indirect TS interference. But the MMSE equalizer introduces both kinds of TS interference as Equation (4.21), where $\mathbf{R}_{uu} = \mathbf{I}_B \otimes (\mathbf{S}\mathbf{A}^2\mathbf{S}^H)$. Similar to the Sections 3.3.2 and 4.4, $\mathbf{R}_u$ can be approximated by

$(A^2Q/M)\mathbf{I}_{N\times N}$ if all users have the same signal amplitude and the TS amplitude satisfies $A_0^2 = A^2Q/M$. Consequently, the same MMSE-FEQ form as Equation (4.24) can be obtained except $\sigma_u^2 = A^2Q/M$ and the scalar form similar to Equation (2.23).

To detect the bits of user 1, the similar de-spread and decision procedures presented in Section 3.2 (cf. Equations (3.3~3.6)) can be applied, where $\mathbf{W}_{FDE}$ should be replaced by $\widehat{\mathbf{W}}_{MMSE}$.

For now, $N_p = 2L+1$ and $N_c = L+1$ are chosen. And the other parameters are summarized in Table 4.4, where $N_u = BM$ and $N_c = L+1 = 8$.

Here only equal transmitted signal amplitude for every active user is concerned. And the TS under the antipodal alphabet constraint is applied and its amplitude $A_0 = A\sqrt{Q/M}$. The Rayliegh fading channels with EQ-PDP and EXP-PDP are chosen similar to Chapter 2, where the vehicle speed is assumed to be 60m/s. As mentioned before, the channel TMSE resulted from the proposed ML channel estimator only depends on the noise variance and TS. Hence, the channel TMSE performance is the same as Figure 4.4.

In the following figures, the lines denoted by "true statistics" represents the situation where $\mathbf{R}_u$ is perfectly known. And "approximated statistics" means that $\mathbf{R}_u$ is approximated by a diagonal matrix mentioned before. Additionally, the performance benchmark is chosen to be the receiver based on the "true statistics" of transmitted signals and known CSI. In this case, no TS is inserted in data frames.

Table 4.4 CP-CDMA System Configuration for Simulation

Spreading factor	16 (= Walsh code length)
Number of active users Q	10 or 16
Chip rate	1.024M chip/s
Carrier frequency	2GHz
Modulation	BPSK
Number of information bits per frame	31 (=B)
Channel length	8 (= L+1)
Frame length for the conventional method	519 ($N_f = N_u + N_p + N_c$)
Frame length for the proposed method	512 ($N_f = N_u + 2N_c$)

4.5.1 Joint Receiver Based on the Conventional Channel Estimation Method

Two aspects of the proposed joint receiver are explored based on the conventional channel estimation method: 1) how much performance loss the joint receiver has if $\mathbf{R}_u$ is approximated through a special diagonal matrix; 2) whether the approximation is still valid when CSI is estimated through the conventional method.

In Figures 4.9 and 4.10, nearly half system loading (Q = 10) is configured over Ralyleigh fading channels with EQ-PDP and EXP-PDP, respectively. Then the answer to two questions is that our approximation is valid for both known CSI and estimated CSI scenarios. And the performance loss due to the approximation is negligible whenever the CSI is estimated or known. This is because CSI has no influence on the approximation of $\mathbf{R}_u$.

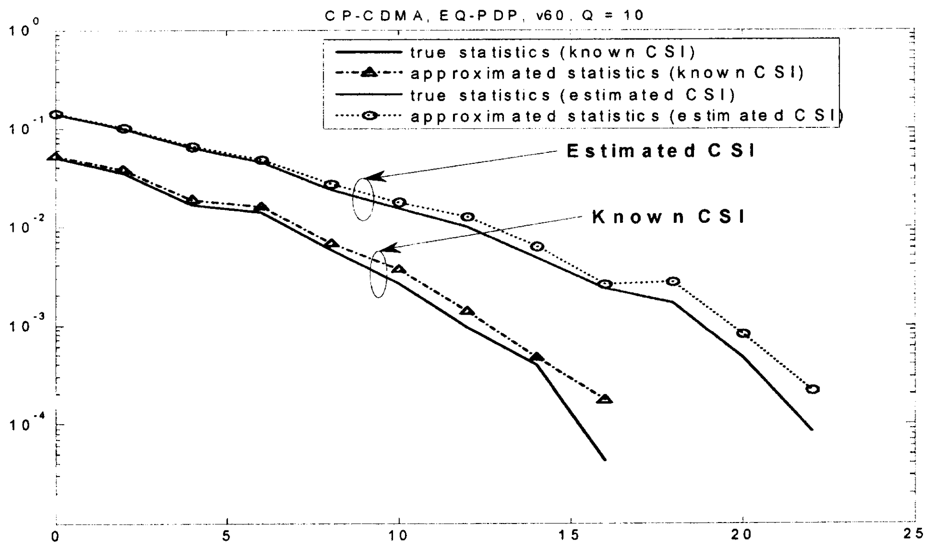

Figure 4.9 BER of joint receiver based on the conventional channel estimator in Rayleigh fading channel with equally PDP (CP-CDMA, $Q = 10$).

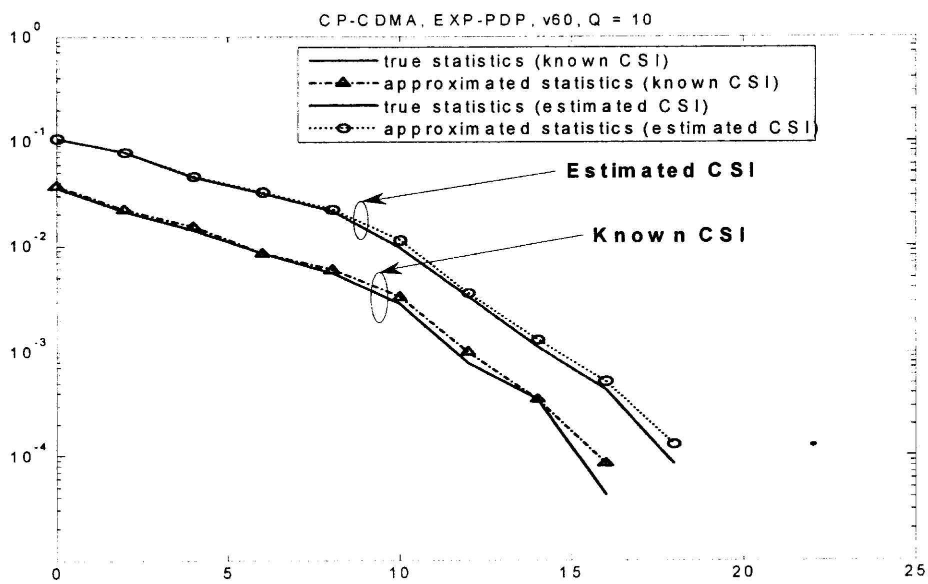

Figure 4.10 BER of joint receiver based on the conventional channel estimator in Rayleigh fading channel with exponentially PDP (CP-CDMA, $Q = 10$).

In Figure 4.11, full system loading (Q = 16) is configured over Ralyleigh fading channels with EQ-PDP and EXP-PDP, respectively. It says that the joint receiver based on the approximated statistics matches MUD based on the true $\mathbf{R}_u$ very well no matter CSI is known or estimated through the conventional method. Compared to Figures 4.9 and 4.10, our claim in Chapter 3 is validated that a diagonal matrix can achieve the better approximation on $\mathbf{R}_u$ for a larger Q.

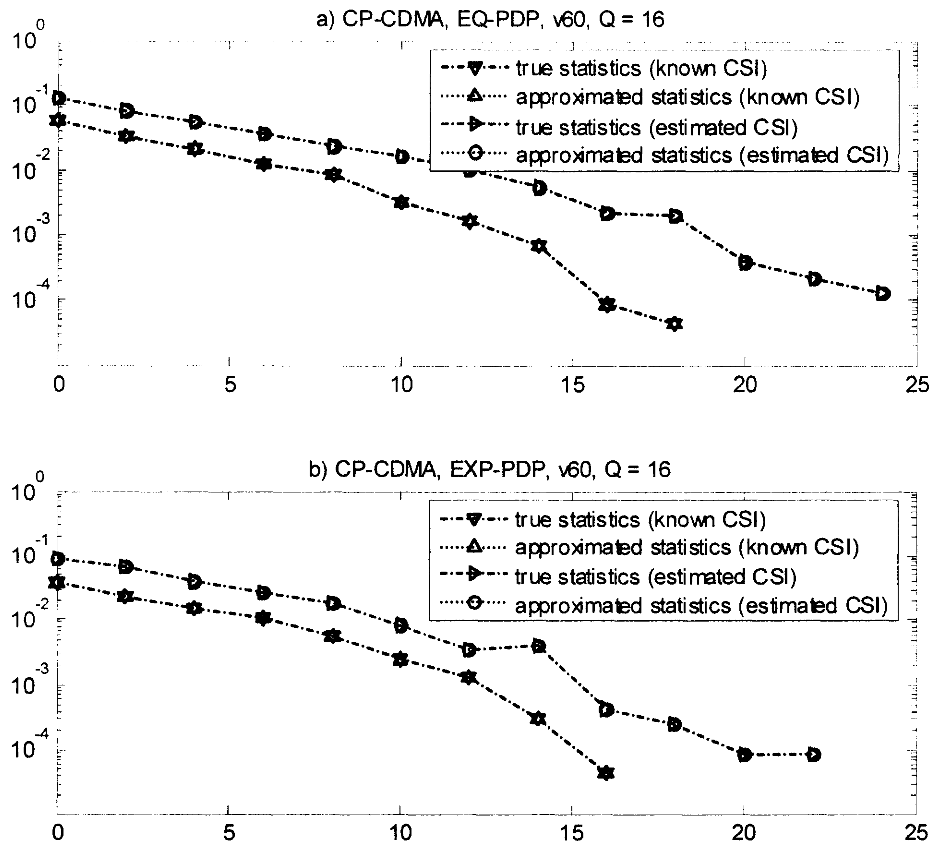

Figure 4.11 BER of joint receiver based on the conventional channel estimator in Rayleigh fading channels (CP-CDMA, Q = 16).

4.5.2 Joint Receiver Based on the Proposed Channel Estimation Method

Since CSI has no impact on the approximation on $\mathbf{R}_u$, such approximation will have the similar property as Section 4.5.1 for the joint receiver based on the proposed channel estimation method. This section focuses on the comparison of the joint receiver based on two channel estimation methods when the approximated $\mathbf{R}_u$ is used.

In Figures 4.12 and 4.13, the conventional method always performs better than the proposed one. According to the conclusion in Section 4.4.3, both methods have similar channel TMSE. For the conventional method, only the channel estimation error degrades the receiver performance if ignoring the additive noise. However, the TS padded in the data block for the proposed method has an additional direct inference, i.e. direct TS interference. It can be seen that the performance gaps between two channel estimation methods are small.

In summary, the proposed frequency domain joint receiver based on the MMSE equalizer and proposed channel estimator can achieve the similar performance as the counterpart based on the conventional estimator for CP-CDMA system. But the proposed channel estimation method has lower system overhead and much lower computational complexity.

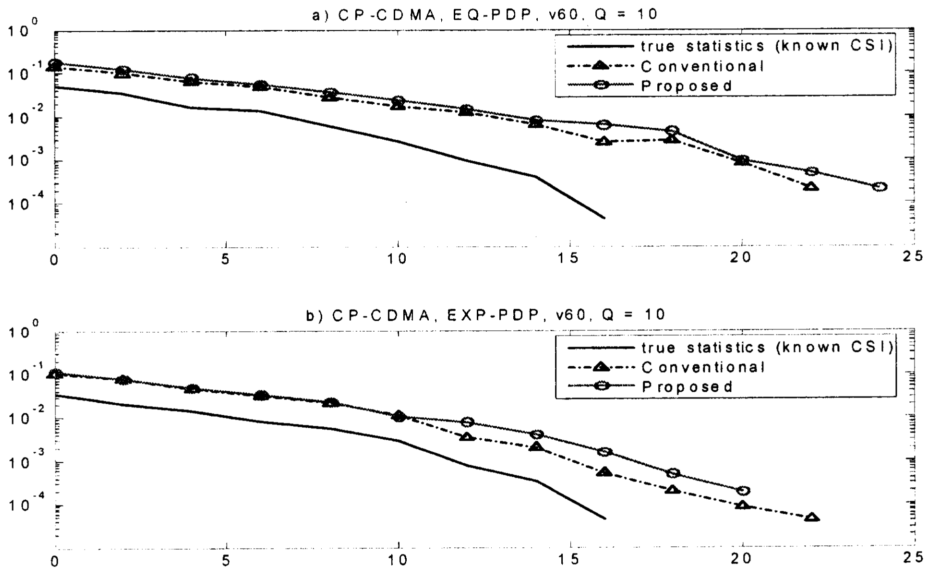

Figure 4.12 BER of joint receiver based on the proposed channel estimator in Rayleigh fading channels (CP-CDMA, $Q = 10$).

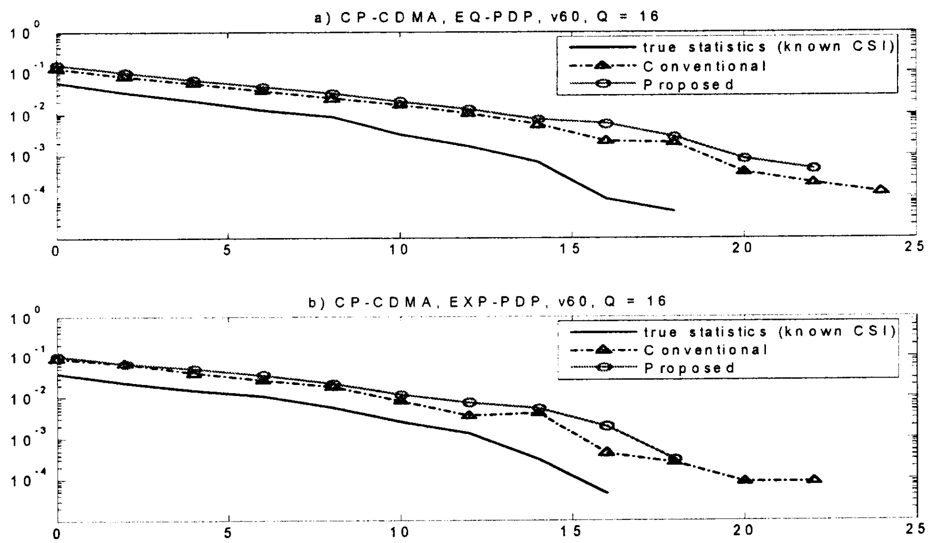

Figure 4.13 BER of joint receiver based on the proposed channel estimator in Rayleigh fading channels (CP-CDMA, $Q = 16$).

CHAPTER 5

CONCLUSION

In this thesis, new channel equalization and estimation methods are studied in cyclic prefix assisted block transmission systems.

Firstly it shows the equivalence of frequency domain and time domain equalization based on zero-forcing criterion as well as for MMSE criterion. In particular, the scalar frequency domain MMSE equalizer is obtained based on an assumption on the independence of transmitted symbols. For CP-CDMA system, a low complexity frequency domain joint receiver is proposed and its performance is studied.

When the FIR channel is unknown to the receiver, a novel channel estimation method is proposed and its performance is studied in comparison with the conventional method. The proposed method has lower system overhead and lower complexity with respect to the conventional method. The design criterion of optimal training sequences for each estimation method is given. Under the antipodal alphabet constraint, it shows that the number of optimal training sequences for the proposed method is much larger than the conventional method.

Lastly, the proposed channel estimator is applied to the BPSK block transmission system and the CP-CDMA system. Simulation results show that the proposed method has similar channel estimation accuracy and leads to similar BER performance, compared to the conventional method.

REFERENCES

1. K.L. Baum, T.A. Thomas, F.W. Vook and V. Nangia, "Cyclic-prefix CDMA: an improved transmission method for broadband DS-CDMA cellular systems", Wireless Communications and Networking Conference, 2002, IEEE, Volume: 1, March 2002.

2. S. Haykin, "Adaptive Filter Theory", Prentice Hall, May 2001.

3. F.C. Zheng, "Optimal training sequences and pilot tones for OFDM systems", Communications Letters, IEEE, Volume: 5, Issue: 4, April 2001.

4. B. Sklar, "Rayleigh fading channels in mobile digital communication systems I. Characterization", Communications Magazine, IEEE, Volume: 35, Issue: 7, July 1997.

5. A. Klein, "Data detection algorithms specially designed for the downlink of CDMA mobile radio systems", Vehicular Technology Conference, 1997 IEEE 47th, Volume: 1, May 1997.

6. L. Deneire, B. Gyselinckx, and M. Engels, "Training sequence versus cyclic prefix-a new look on single carrier communication", Communications Letters, IEEE, Volume: 5, Issue: 7, July 2001.

7. J.H. Manton, "Optimal training sequences and pilot tones for OFDM systems", Communications Letters, IEEE, Volume: 5, Issue: 4, April 2001.

8. L. Martoyo, T. Weiss, F. Capar and F.K. Jondral, "Low complexity CDMA downlink receiver based on frequency domain equalization", Vehicular Technology Conference, 2003. VTC 2003-Fall. 2003 IEEE 58th, Volume: 2, October 2003.

9. Z. Wang, G.B. Giannakis, "Wireless multicarrier communications: where Fourier meets Shannon", IEEE Signal Processing Magazine, Volume: 47, Issue: 3, May 2000.

10. J.G. Proakis, "Digital Communications", McGraw-Hill Education, December 2000.